General Disclaimer

One or more of the Following Statements may affect this Document

- This document has been reproduced from the best copy furnished by the organizational source. It is being released in the interest of making available as much information as possible.

- This document may contain data, which exceeds the sheet parameters. It was furnished in this condition by the organizational source and is the best copy available.

- This document may contain tone-on-tone or color graphs, charts and/or pictures, which have been reproduced in black and white.

- This document is paginated as submitted by the original source.

- Portions of this document are not fully legible due to the historical nature of some of the material. However, it is the best reproduction available from the original submission.

X-690-71-23
PREPRINT

NASA TM X- 65436

OBSERVATIONS OF THE INTERPLANETARY MEDIUM: VELA 3 - IMP 3 1965-1967

N. F. NESS
A. J. HUNDHAUSEN
S. J. BAME

JANUARY 1971

GSFC
GODDARD SPACE FLIGHT CENTER
GREENBELT, MARYLAND

X-690-71-23

OBSERVATIONS OF THE INTERPLANETARY MEDIUM:

VELA 3-IMP 3, 1965-1967

N. F. Ness
Laboratory for Extraterrestrial Physics
NASA-Goddard Space Flight Center
Greenbelt, Maryland

A. J. Hundhausen
S. J. Bame
Los Alamos Scientific Laboratories
Los Alamos, New Mexico

November 1970

ABSTRACT

Simultaneous observations of the interplanetary plasma by the Vela 3 satellites and the interplanetary magnetic field by the IMP 3 satellite from July 1965 to July 1967 are presented. Pertinent derived plasma properties are computed and statistically tabulated. The quiet solar wind, $300 \leq V \leq 350$ km/sec, is found to be represented by an average field strength of 4.7γ at $\phi_{SE} = 137^{\circ}$ (317°), $\theta_{SE} = -3.2^{\circ}$ with significant variations. The ratio of plasma ion energy density to magnetic field energy density averages 1.2, with an average β_p of 0.78. The average Alfvén speed is drived to be 36 km/sec which yields a Mach flow of 10.7. The solar wind plasma most frequently is stable with respect to the firehose mode of instability. The existence of an evolutionary sector geometry does not destroy the pattern of correlated variation of plasma and field parameters observed within the sectors although the distortion of sectors by propagating shock waves is suggested.

INTRODUCTION

Both the interplanetary plasma and magnetic field have been extensively studied using spacecraft-borne instruments, and their general features are well-known (see recent reviews by Dessler (1967), Ness (1967, 1969) Axford (1968), Hundhausen (1968, 1970) and Wilcox (1968)). The properties of field and particles would be expected to be closely related, both because of their common solar origin and because of the general coupling of the magnetic field and charged particles in a plasma. Some such relationships have been observed (e.g., the occurrence of magnetic sectors within high-speed plasma streams, the alignment of proton thermal anisotropies with the magnetic field direction, and the existence of nearly simultaneous, discontinuous changes in magnetic field and plasma properties)

This paper will describe the results of an extensive comparison of solar wind proton properties observed on the twin Vela 3 satellites with magnetic field properties observed on the IMP 3 satellite. It is thus an extension of the study of thermal anisotropies given by Hundhausen, Bame and Ness (1967c) and is in many ways similar to the comparison, involving Mariner 2 data, presented by Neugebauer and Snyder (1967). A statistical analysis of field, particle, and combined parameters will emphasize proton thermal properties. Relationships among the variations in field and particle parameters will be described, and the sector-high speed stream pattern discussed.

1. OBSERVATIONAL BACKGROUND

The Vela 3 plasma observations were made with a previously described electrostatic analyzer system (Bame et al., 1967; Gosling et al., 1967, Hundhausen et al. 1967a, 1967b). Plasma properties used herein were derived from the flux data by the least square fitting of bi-Maxwellian distribution functions, as described in Hundhausen, Bame, Asbridge and Sydoriak, (1970a), hereafter referred to as HBAS. This analysis yields the following proton properties from each 4.27 minute data cycle, assuming a symmetrical distribution function about the plane of analysis (see HBAS)

N, the proton density

V, the flow (or solar wind) speed

φ, the flow direction (in solar ecliptic longitude)

T, the proton temperature (an average over the anisotropic distribution)

K, the ratio of maximum to minimum temperatures for the anisotropic distribution

ψ, the direction of maximum temperature anisotropy

A statistical analysis of these properties based on Vela 3 observations from July 1965 to mid-1967 has been given in HBAS.

The IMP 3 magnetometer has been described by Ness and Taylor (1968) and by Taylor (1969). The magnetic field vectors used herein are 5.46 minute averages, thus comparable to the cycle time of the Vela plasma detector. The magnetic field is described by the parameters

B, the field magnitude

ϕ, the solar ecliptic longitude of the projection of $\vec{B}$ onto the ecliptic plane

θ, the angle between $\vec{B}$ and the ecliptic plane, positive North of ecliptic

As solar wind conditions are rarely steady, a correction must be made for the different arrival times of a particular field line at the two satellites. Figure 1 shows an IMP 3 position (X_I, Y_I) and a Vela 3 position (X_V, Y_V) projected on the ecliptic plane. We assume that the field configuration is stationary (on the time scale necessary for transit at the solar wind speed between the satellites) in a frame of reference moving with the solar wind. A magnetic field line swept past IMP 3 at t_I will then arrive at Vela 3, assuming $\varphi = 180^\circ$, at

$$t_V = t_{IMP} + \frac{X_I - X_V + (Y_I - Y_V) \cot \phi}{V}$$

A magnetic field observation $B(t_I)$ is considered to have been observed "simultaneously" with a set of plasma parameters if the predicted time t_V falls within the plasma data acquisition cycle. As V is actually observed only at the Vela spacecraft, an iterative solution for t_V was necessary. Large transit times associated with angles ϕ near 0° or 180° were avoided by discarding any observations with transit corrections larger than an hour. This correction procedure for the convection of the solar wind past the two satellites assumes that the field lines are straight and the structure is independent of distance from the ecliptic plane, on the scale of the spatial separation of the two satellites.

2. SOLAR WIND CONDITIONS DURING THE PERIOD OF STUDY

Of the 13,976 sets of solar wind plasma parameters derived from Vela 3 data obtained between July 1965 and mid-1967 and discussed in HBAS, 4336 could be matched with "simultaneous" IMP 3 solar wind magnetic field parameters by the procedure described in Section 2. Of these, 3002 observations or 70% occurred between 24 July 1965 and 8 February 1966; 1334 occurred between 15 July 1966 and 18 January 1967. During the intervening period IMP 3 was generally not in the interplanetary medium (Taylor, 1969). Table 1 gives the average values of five plasma properties, based on the subset of 4336 simultaneous observations, the medians and RMS deviations (σ) and the 5-95% percentile ranges. Comparison with the averages from the entire period of Vela 3 data acqusition (Table 2 of HBAS) reveals that this subset is in no way atypical. Figure 2 shows histograms of B, ϕ, and θ from the 4336 simultaneous IMP 3 observations. Comparison with histograms of the magnetic fields observed on other spacecraft (e.g., Ness and Wilcox (1964), Fairfield and Ness (1967), Ness (1969)) again reveals no atypical features. The tendency for the field to point predominantly inward towards the sun is in agreement with observations from these same periods described by Rosenberg and Coleman (1969).

3. STATISTICAL DISTRIBUTION OF PLASMA PROPERTIES

A number of important plasma parameters require knowledge of both particle and magnetic field properties. The following will be considered here:

Ratio of magnetic and proton thermal energy densities

$$\epsilon = \frac{B^2}{8\pi} \Big/ \left(\frac{3}{2}\ NkT\right)$$

Proton beta, $\beta_p = NkT \Big/ \frac{B^2}{8\pi}$ (3.1)

Alfvén speed, $V_A = \left(\frac{B^2}{4\pi NM}\right)^{1/2}$, where M is the proton mass.

Alfvén Mach number, $M_A = V/V_A$

Firehose stability parameter, $\alpha_p = \frac{NK(T_{\parallel} - T_{\perp})}{B^2/4\pi}$

(where $T_{\parallel}$ ($T_{\perp}$) is temperature parallel (transverse to B.)

Angle between maximum proton temperature and magnetic field, $\Delta = \phi - \psi_B$,

(where ψ_B is the direction of B projected into the Vela analysis plane) (see Hundhausen et al., 1967c). The statistical distributions of these parameters will be presented. For reference purposes, Table 2 summarizes these distributions with the standard statistical quantities of Table 1.

3.1 Energy Densities:

Figure 3 shows separate histograms of the logarithms of the proton thermal energy density derived from Vela 3 observations and the magnetic energy density derived from the simultaneous IMP 3 observations.

These logarithmic distributions are nearly symmetric and could be quite well approximated by normal distributions. This property of the distributions of many solar wind parameters has been discussed in HBAS (we note the implication that the distribution of log B must also be approximately normal; a direct test confirms this expectation).

The two histograms of Figure 3 show strong similarities: the two energy densities lie in nearly the same range, have very nearly the same average, and have only slightly (8%) different standard deviations. Figure 4 shows the histogram of the energy density ratio ε. A linear display has been chosen to explicitly show the skewness of the distribution. As might be expected from Figure 3, the average ratio is near one; $\langle \varepsilon \rangle = 1.01$. Neugebauer and Snyder (1967) reported a similar near equality of magnetic and ion (i.e., including the approximate 20% additional energy in He^{++} ions) thermal energy densities observed on Mariner 2.

The Mariner result was interpreted as an equi-partition of energy in the presence of small-amplitude hydrodynamic waves. Two cautionary comments should be made regarding the physical interpretation of this equipartition: (1) the result depends on the difficult absolute calibration of the plasma detector. As different plasma detectors have sometimes observed widely different densities, such calibrations may not be well known (see HBAS for an evaluation of the Vela 3 calibration); (2) although $\langle \varepsilon \rangle$ is near one, the distribution of ε shows both a wide spread ($\sigma/\langle \varepsilon \rangle = 0.79$) and a large skewness. It should also be emphasized that under quiet solar wind conditions, the electrons are observed directly to be three or four times as hot as the protons (Bame et al., 1969) and indirectly to be approximately

twice as hot (Ogilvie and Ness, 1969). Thus the total thermal energy density in the plasma must be at least several times larger than the magnetic field energy density. A similar conclusion has been arrived at by Burlaga and Ogilvie (1970b).

3.2 Proton Beta: β_p

The quantity $\beta_p = \frac{P}{B^2/8\pi}$ (where P is the pressure) is often used in plasma physics to describe the partition of energy between particles and magnetic field. Only the proton beta, $\beta_p = \frac{NkT}{B^2/8\pi}$ (where T is the proton temperature) can be derived from the data under discussion. The average value of the latter is $\langle \beta_p \rangle = 0.95$; the most probable value is near 0.6. Burlaga and Ogilvie (1970b) obtained a most probable β_p of 0.3 and β_{p+e} of 1.0 from Explorer 34 observations made in late 1967. The most likely reason for the difference between the Vela 3 and Explorer 34 values is the density calibration already mentioned above; the densities derived from the latter observations are generally lower than derived from the former (compare the density histograms in Ogilvie (1970) and HBAS). Inclusion of the electron contribution will give a substantially different total β, about three times larger than β_p i.e., $\beta_{p+e} = 3.0$.

3.3 Alfvén Speed: V_A

Figure 5 shows the histogram of Alfvén speeds derived from the Vela-IMP data. These results compare reasonably well with those of Neugebauer and Snyder (1967), with some tendency for smaller values in the present analysis. The average value $V_A = 43$ km/sec agrees very well with the value of 41 km/sec deduced by Whang and Ness (1970) from the geometry of the lunar Mach cone.

3.4 Alfven Mach Number: M_A

The average Alfven Mach number derived from the Vela 3-IMP 3 data is $M_A = 10.7$. The average sonic Mach number derived from Vela 3 data (HBAS) is 9.5. These averages and the lower limits on the 5 to 95 percentile ranges: 5.6 for M_s and 4.4 for M_A again confirm the supersonic nature of the solar wind. M_A is found to be less than 2 for only 14 of these 4336 individual observations. Neugebauer and Snyder (1967) found that the Alfven Mach number derived from the 3-hour averages of V and V_A never fell below two. Similar results have been obtained from the Explorer 34 data (Fairfield, 1970).

3.5 Thermal Anisotropy and Magnetic Field Orientation: ψ, ψ_B

The angle ψ, that gives the direction of maximum temperature of the assumed bi-Maxwellian proton distribution function, is defined in the Vela plane of analysis. This plane contains both the sun-satellite line and the common normal to the sun-satellite line and the satellite spin axis. Let ψ_B be the direction of the projection of B onto this plane. Figure 6 shows the observed distribution of $\Delta = \psi - \psi_B$ ($-90^\circ \leq \Delta \leq 90^\circ$ because ψ and $\psi \pm 180^\circ$ are completely equivalent). The distribution has a pronounced peak near $\Delta = 0$ with a RMS width of 38°; 58% of the observations fall in the range $-30^\circ \leq \Delta \leq 30^\circ$. The alignment of maximum proton temperature with the magnetic field (Hundhausen et al., 1967c) for which $\Delta = 0$, is generally confirmed by this peak in the distribution. However, the nearly constant fraction of observed values in angular intervals with $\Delta < 60^\circ$ may indicate that the maximum temperature and magnetic field are not always aligned. An alternate explanation is a breakdown in precise coherence between the magnetic field

directions at IMP 3 and Vela 3 in the presence of waves propagating upstream from the earth's bow shock. This phenomenon was found to exist and produce such an effect in Hundhausen et al. (1967c). For observations of these waves, see Fairfield (1969) and Greenstadt et al. (1968).

The distribution function determined from Vela 3 data is projected on the plane of analysis. If the distribution function is, as expected, symmetric about B with the maximum temperature in the direction of B, the observed T_{max} is the projection on this plane of the actual temperature $T_{\parallel}$ along the field line. The true anisotropy ratio $K_t = T_{\parallel}/T_{\perp}$ is related to the observed $K = T_{max}/T_{min}$ by

$$K_t = \frac{K}{\cos \Theta}$$

where Θ is the angle between B and the plane of analysis. For the 2500 Vela-IMP observations with $\Lambda \leq 30^{\circ}$ (i.e., reasonable alignment), $K = 1.67$, while $K_t = 1.94$. The correction to the average for the projection effect is only 16% for this sample.

3.6 Firehose Stability Criterion: α

In the magnetohydrodynamic or long wavelength limit, the firehose instability occurs for

$$\alpha = \frac{Nk\,(T_{\parallel}-T_{\perp})}{B^2/4\pi} > 1$$

(e.g., Parker (1963), Longmire (1963)). As only proton temperatures are available from the data under discussion, only the proton contribution α_p to this stability criterion can be evaluated. Figure 7

shows the histogram of observed values of α_p for the 2500 cases with $\Delta \leq 30^\circ$. The average value is $\langle \alpha_p \rangle = 0.48$, while $\alpha > 1$ for only 18% of the observed values. We thus conclude that the proton anisotropies are only rather infrequently large enough to excite the firehose instability, and that this instability probably does not play a significant role in limiting the growth of proton anisotropies. Similar conclusions were reached by Scarf et al. (1967) on the basis of a single observation and by Eviator and Schulz (1970) on the basis of several intervals of Vela 4 data.

The firehose instability could still occur, however, if the electron contribution to α were large enough (Hundhausen et al., 1967a, 1967c). However, solar wind electron observations (Montgomery et al., 1968; Bame et al., 1969) indicate that, although the electron temperature is significantly higher (generally near 1.5×10^5°K) than the proton temperature (so that the electron pressure will dominate α), the electron thermal anisotropy is small, with $T_{//}/T_{\perp} < 1.2$. For an average density of 7 electrons cm^{-3} and the average magnetic energy density $B^2/8\pi \sim 10^{-10}$ ergs cm^{-3} from Figure 3,

$$\alpha \approx 0.96$$

It thus appears doubtful that even the additional contribution to α from electron anisotropies will normally lead to the firehose instability. A similar conclusion has been reached by Eviator and Schulz (1970). However, one cannot exclude the possibility that the firehose instability might occur locally on occasions (Burlaga et al., 1969).

4. RELATIONSHIPS AMONG PLASMA PROPERTIES

Solar wind properties are observed to vary widely. It is well-known that some of these variations are not independent; e.g., proton temperature and flow speed are directly and strongly correlated (Neugebauer and Snyder, 1966; Strong et al., 1966; Coon, 1968; Burlaga and Ogilvie, 1970a; HBAS). In discussing relationships among the solar wind parameters derivable from the Vela 3-IMP 3 data, we follow HBAS and Burlaga and Ogilvie (1970). One solar wind property will be regarded as an independent variable and the dependence of another property upon this variable discussed in terms of the statistical quantities already used in Table 2. A standard choice for one independent variable is the flow speed, V, which reflects the widely accepted identification of low flow speeds with quiet or undisturbed conditions and high flow speeds with disturbed conditions (see the review by Hundhausen 1970).

4.1 The Magnetic Field-Flow Speed Relationship

Figure 8 shows the average magnetic fields computed separately for the flow speed intervals $250 \leq V \leq 300$ km sec^{-1}, $300 \leq V \leq 350$ km sec^{-1}, etc. The vertical bars indicate the standard deviations within each interval. The standard errors in the averages range from 8% (in the $250 \leq V \leq 300$ km sec^{-1} range) to 3% (in the $300 \leq V \leq 350$ km sec^{-1} range) of the standard deviations (in the approximation that the distributions are normal and all observations are independent). The only strong dependence of magnetic field on flow speed indicated from these data is a $\approx$30% decrease in B at low flow speeds. The statistial significance of this effect is questionable; only 173 observations were made in the $250 \leq V \leq 300$ km sec^{-1} interval, and over half of these occurred

on two days. We can safely conclude, however, that the average dependence of field magnitude on flow speed is small over the range $300 \leq V \leq 600$ km sec^{-1} in which 96% of the Vela 3-IMP 3 observations were made. A similar conclusion, based on the Explorer 34 data, has been published by Burlaga and Ogilvie (1970).

4.2 The Magnetic Field-Plasma Density Relationship

Figure 9 shows the average magnetic field computed separately for the density intervals $0 \leq N \leq 2$ cm^{-3}, $2 \leq N \leq 4$ cm^{-3}, $4 \leq N \leq 6$ cm^{-3}, etc., the vertical bars indicate the standard deviations within each interval. Very little dependence of B on the density is indicated. The high average field in the $0 \leq N \leq 2$ cm^{-3} interval is based on only 38 observations, and is thus probably not statistically significant. High magnetic fields are associated with the high densities occurring where high velocity solar wind streams overtake slower streams (Neugebauer and Snyder, 1967), or near sector boundaries (Wilcox, 1968), or behind interplanetary shock waves (Hirshberg et al., 1969). The absence of any strong trend to high fields at large densities in Figure 9 indicates that such transient events have little effect on long term averages.

4.3 Magnetic Field Direction-Flow Speed Relationship

The interplanetary magnetic field is "frozen" into the high conductivity coronal and interplanetary plasma, and is expected to be drawn into a spiral configuration by the radial plasma flow and the rotation of the sun (see Parker, 1963; Ahluwalia and Dessler, 1962). Near the earth, this idealized model predicts field lines lying nearly in the ecliptic plane and at the angle

$$\phi = \tan \frac{\Omega r}{V} \qquad (1)$$

(where Ω is the angular speed of solar rotation, r is the heliocentric distance) from the radial. Numerous observations (e.g., Ness and Wilcox 1964; Ness, 1967) have revealed an average interplanetary field in basic agreement with this prediction; i.e., pointing at a solar ecliptic latitude near 0° and at a solar ecliptic longitude near the 135° or 315° implied by equation (1) with $V = 400$ km sec^{-1}.

Figure 10 shows the average solar ecliptic longitudes of the magnetic field lines (i.e., with the solar ecliptic longitudes of the vector field converted into the range $45^\circ \leq \psi \leq 225^\circ$) computed from IMP 3 data for the flow speed intervals $250 \leq V \leq 300$ km sec^{-1}, $300 \leq V \leq 350$ km sec^{-1}, etc. The vertical bars again show the standard deviations in each interval. The dashed line shows the solar ecliptic longitude as a function of flow speed predicted by equation (1). Although each average longitude agrees roughly with the prediction, there is no trace of the expected variation with flow speed. A similar result was obtained by Neugebauer and Snyder (1967) from Mariner 2 data. The average ecliptic latitudes of the field lines in these same intervals lie between -6.1° and 11.3°. Again no trend is discernable.

Thus, although the observed average field configuration is close to that predicted by the "frozen-in" model, the expected changes in this configuration with changing flow speed are not observed. Neugebauer and Snyder (1967, p. 1827) attributed this failure of the model to "the distortion of the underlying spiral pattern by waves or other disturbances." This observation confirms the conclusions of earlier workers, that the solar wind cannot, in general, be described by models which assume a steady, spherically-symmetric flow of plasma from the sun.

4.4 The Proton Beta-Flow Speed Relationship

Figure 11 shows the average β_p (Section 3.2) in the now familiar 50 km sec^{-1} flow speed intervals. The standard deviations within these intervals are all slightly larger than the averages. Despite these large variations, there is a significant dependence of β_p on the flow speed. β_p is smallest for $300 \leq V \leq 400$ km sec^{-1}, rising with increasing flow speed for $V > 400$ km sec^{-1}. This rise is primarily the result of the high proton temperatures observed at high flow speeds. β_p is also higher in the $250 \leq V \leq 300$ km sec^{-1} interval. This is primarily the result of the low magnetic field strength (and high density) and is subject to previously mentioned questions of statistical significance.

Burlaga et al. (1969) have shown that magnetic field flucutations with periods in the range 1 minute to 1 hour are related to the proton beta. For $\beta_p < 1$, the magnetic field is generally quiet; for $\beta_p > 1$, the magnetic field shows increased fluctuations. Figure 11 then leads to the expectation of quiet magnetic fields at low flow speeds and disturbed magnetic fields at high flow speeds. This gives still another indication of the disturbed nature of the solar wind observed at high flow speeds.

4.5 "Spectral Temperature" - Magnetic Field Direction Relationship.

Proton temperatures are often derived from position ion energy spectra. If the maximum temperature of the anisotropic proton distribution is aligned with the magnetic field (as inferred in Section 3.5), and if there is no compensating correlation between the maximum temperature and the magnetic field orientation, then this "spectral temperature" should depend upon the magnetic field orientation. When the magnetic

field points in the radial direction, the spectral temperature should equal the maximum (or parallel) temperature. Correspondingly when the magnetic field points in the azimuthal direction, the spectral temperature should equal the minimum or transverse temperature.

Although no true spectral temperatures have been directly derived in the Vela 3 data analysis, a closely related quantity is the temperature in the radial direction implied by the bi-Maxwellian distribution function. Figure 12 shows this radial temperature as a function of the solar ecliptic longitude of the magnetic field for cases in which $\Delta \leq 30^{\circ}$ (i.e., good alignment). The expected relationship is strongly indicated; the radial temperature is highest when the field points in the radial direction. Neugebauer and Snyder (1967) found no such relationship between the spectral temperature derived from Mariner 2 data and the longitude of the magnetic field, concluding that if a field aligned anisotropy were present, the maximum temperature must be dependent on the field direction. A direct examination of the maximum temperature derived from the Vela data and the field orientation reveals only a weak relationship which, if real, would slightly increase the dependence of spectral temperature on field orientation.

4.6 Alfvén Mach Number - Flow Speed Relationship

The average Alfven Mach numbers, computed with 50 km sec^{-1} flow speed intervals, all lie between 10.2 and 12.1 for $300 \leq V \leq 600$ km sec^{-1}. A higher value, $M_A = 14.1$, is obtained for $250 \leq V \leq 300$ km sec^{-1}, this results from the low B in this interval and is again subject to the same arguments concerning statistical significance as in Section 4.1. For V >300 km sec, or 96% of the solar wind observations, M_A is almost

independent of V. This lack of dependence results from an inverse dependence of N on V (HBAS; Neugebauer and Snyder, 1967; Burlaga and Ogilvie, 1970).

5. PROPERTIES OF THE QUIET SOLAR WIND

Many observers (Neugebauer and Snyder, 1966; Strong et al., 1966; Hundhausen, 1970; HBAS) have related quiet conditions in the solar wind (i.e., the relative absence of variations produced by spatial structures or temporal changes) with low solar wind speeds. As in HBAS, we will use the flow speed interval 300 to 350 km sec^{-1} as the criterion for quiet solar wind. Table 3 summarizes the magnetic fields and plasma parameters observed in this interval.

6. PLASMA VARIATIONS RELATED TO MAGNETIC SECTORS

The directional sense of the interplanetary magnetic field is observed to vary with time in a highly systematic manner. Regions of a single dominant magnetic polarity, with B pointing away from or toward the sun (along the average spiral orientation), persist for periods of the order of several days, apparently corotating with the solar atmosphere. These "magnetic sectors" have been identified in observations extending over most of the solar cycle (Wilcox and Ness, 1965; Coleman et al., 1967, 1967; Ness and Wilcox, 1967; Wilcox and Colburn, 1969, 1970). The boundaries of magnetic sectors has also proven useful in organizing the variations observed in plasma properties (Wilcox, 1968). At the passage of a sector boundary the flow speed is generally found to be low (near 300 km sec^{-1}), rising thereafter, and attaining a maximum value within 2 days. The magnetic field intensity follows a similar pattern. The plasma density is found to reach a maximum value shortly after the sector boundary, with a rapid decrease occurring while the flow speed remains high. This pattern of variations, similar to that to be expected where a fast solar wind stream overtakes a slow stream,

was found to be most regular in the IMP 1 observations of late 1963 (Wilcox, 1968), less regular in the Mariner 2 observations of late 1962 (Neugebauer and Synder, 1967).

The Vela and IMP data under discussion here were obtained during the rising portion of the present solar cycle. The magnetic sector structure during this period has been studied by Ness and Wilcox (1967) using IMP 3 data and by Wilcox and Colburn (1969) using Explorer 33 and 35 data. The former found a rapid evolution of the sector pattern to begin in 1965 in contrast to the quasi-stationary pattern, repeating on successive solar rotations, observed by Mariner 2 in late 1962, IMP 1 in late 1963, and IMP 2 and Mariner 4 in late 1964. Wilcox and Colburn (1969, P2388) found that, in 1966 and 1967, the sector pattern was "often quasi-stationary for a few solar rotations, followed by an appreciable change in the next rotation." Both studies attributed the observed evolution of the sector pattern to the development of activity in the new solar cycle.

We have examined the variations in the Vela-IMP plasma properties within the magnetic sectors already given by Ness and Wilcox (1967) and Wilcox and Colburn (1969). As might be expected in view of the rapid evolution of the sectors during this period, these variations are not as regular as those described by Wilcox (1968). However, if attention is centered on those sector boundaries which fit the criterion for "well-established" boundaries by Wilcox and Colburn (1969), i.e., that the magnetic polarity remain unchanged for four days before and four days after the change at the boundary, the familiar pattern emerges. Figure 13 is a superposed plot of three hour averages of the flow speed, proton density, proton temperature, and magnetic field strength as

a function of time relative to the 11 well-established sector boundaries which occur during the period of this study. Both the three-hour averages and the standard deviation of the individual three-hour averages are shown for each interval. The flow speed, proton temperature, and magnetic field strength all begin to rise very near the sector boundary, while the proton density rises somewhat earlier and peaks near the boundary. The flow speed and proton temperature continue to rise for several days, reaching maximum values well into the new sector. These variations closely resemble those described by Wilcox (1968). However, the large standard deviations within many three-hour intervals indicate considerable departure from the regular pattern. In fact, for two of the seven well-established sector boundaries given in Wilcox and Colburn and for which Vela 3 plasma data is available, the expected pattern of plasma variations is definitely not observed.

The variation in flow direction shown in Figure 13 deserves special comment. A clear tendency is present for the flow to shift to a negative direction (from east of the sun) 1 to 2 days before arrival of the sector boundary, and to then change to a positive direction(from west of the sun) at the boundary with the westerly flow persisting for 1 or 2 days. A similar pattern has been observed by Lazarus (1970) in observations made with the Pioneer 6 and 7 spacecraft. This variation in flow direction is in basic agreement with the predictions of Carovillano and Siscoe (1969) for the deflections at the interface between steady, corotating solar wind streams.

7. THE REAL SOLAR WIND: SOLAR ROTATIONS

Further insight into the variations of plasma parameters within magnetic sectors can be gained from Figures 14, 15 and 16. These graphs show three-hour averages of the flow speed, proton density, proton temperature, and magnetic field strength as functions of time for the first three solar rotations after the Vela 3 launch, along with the magnetic polarities given in Ness and Wilcox (1967). The expected pattern of variations in plasma parameters is followed at nearly every change in magnetic polarity during these three solar rotations (e.g., July 27, August 18-19, September 16 and September 22-23). The same pattern of plasma variations indicating the presence of a high-speed stream, occasionally occurs within a magnetic sector (e.g., September 4). The Mariner 2 observations of 1962 revealed more than one high speed stream within the quasi-stationary magnetic sectors present at that time (Coleman et al.,1967).

Five interplanetary shock waves can be identified in the Vela 3 data during these three solar rotations; discontinuous changes in the magnetic field observed on IMP 3 were reported for each of these events by Taylor (1969). These five shocks are indicated along the flow speed curves of Figures 14-16 by vertical lines and the letter S. Three of these shocks (August 18, August 23, and September 15) occur near sector boundaries. Wilcox and Ness (1967) and Wilcox and Colburn (1969) noted the occurrence of several sudden commencements of geomagnetic activity near sector boundaries, and the latter concluded that "a sudden commencement is not necessarily associated with a flare-induced shock wave, but may also be caused by a corotating sector boundary".

The present results might also be regarded as evidence for this conclusion. However, it is by no means clear that the observed shock waves are actually corotating. For example, Taylor (1969) shows a normal for the September 15 shock that is not consistent with the direction expected for a corotating surface (Hundhausen, 1970). In fact, the interplanetary shock waves that produced two of the three sudden commencements upon which Wilcox and Colburn based the conclusion quoted above have been directly observed and in fact identified as flare-associated (Bame et al., 1968; Hundhausen et al., 1970b).

We believe that three possibilities for the nature of such shocks exist: (1)corotating and related to the presence of a quasi-stationary fast solar wind stream, (2) flare-associated disturbances propagating within an already existing quasi-stationary sector structure, or (3) flare-associated disturbances that have severely distorted a pre-existing sector structure. The two latter possibilities have been discussed for a July 1966 shock wave by Lazarus and Binsack (1969) and Ness and Taylor (1969). The present authors believe that (3) represents a more plausible cause for the observed correlation of some sudden commencements with sector boundaries.

The two remaining shock waves (September 12 and September 26) occur within large and previously stable negative sectors; the shocks are followed by short periods of positive polarity. These events probably represent shortlived modifications of an existing sector pattern by flare-ejected material propagating through interplanetary space.

8. CONCLUSIONS

A statistical study of simultaneously obtained interplanetary plasma data from the Vela 3 satellites and interplanetary magnetic field data observed by IMP 3 have confirmed earlier studies of the general properties of the extended solar corona as observed at 1 AU. A detailed correlation of relevant plasma parameters suggest that the interplanetary medium is not a magnetized plasma in which equi-partition of energy exists between the plasma and magnetic field. Rather the thermal energy density of the plasma considering both (ions and electrons) appears to be a factor of 3 or more greater than the magnetic field energy density

Computation and statistical studies of various derived magnetic field-plasma parameters reveal that the solar wind plasma is stable against such instabilities as the firehose mode. The solar wind flow is demonstrated to be highly supersonic, greater than Mach 4.4 for 95% of the observing time.

The relationship of high velocity streams, sector boundaries, sudden commencement storms and interplanetary shocks has been briefly studied with these data. It is concluded that the near simultaneous occurrence of sudden commencement storms with sector boundaries is not necessarily an intrinsic property of a sector boundary itself. Rather the distortion of a quasi-stationary sector pattern by a solar originated transient disturbance (a propagating shock wave) leads to the sequence of events in which near coincidence of such terrestrial disturbances is correlated with sector boundaries. The earlier

established correlation between variation of plasma properties within a quasi-stationary sector is evident and observed in non-active sectors in 1967-1967.

It appears that the solar wind flow velocity, V,is a prime candidate for the principal independent parameter. Correlated variations of directions of the flow velocity with variations in the magnitude are consistent with the solar wind being a composite of high velocity streams overtaking slow velocity streams. In summary, the interplanetary medium appears to represent a suite of plasma streams originating from different regions on the sun with varying time histories some of which evolve at a considerably more rapid rate during periods of solar activity than during periods of minimum activity.

ACKNOWLEDGEMENTS

We appreciate the support and cooperation of our colleagues at Los Alamos Scientific Laboratories and NASA-Goddard Space Flight Center in the conduct of these experiments and the analysis of these data.

The Vela portions of the data were obtained as part of the Vela nuclear test detection satellite program, a joint program of the Advanced Research Projects Agency of the U. S. Department of Defense and the U. S. Atomic Energy Commission. The program is managed by the U. S. Air Force.

TABLE 1

AVERAGE PLASMA PARAMETERS FOR THE PERIOD OF STUDY

Property	Average	Median	σ	Range
N	7.0 cm^{-3}	6.5	3.3	3.0 to 14.7
V	412 km sec^{-1}	405	72	305 to 55
T	8.0 x $10^{4}{}^{o}K$	$7.5X10^{4}$	$4.0x10^{4}$	$2x10^{4}$ to $2.4x10^{5}$
K	1.67	1.64	.47	1.1 to 3.7
ψ	129^{o}	--	38^{o}	--
B	5.2γ	4.2	2.4	2.2 to 9.9

TABLE 2

DERIVED SOLAR WIND PLASMA PARAMETERS

Parameter	Average	Median	σ	Range
ϵ	1.01	0.82	0.80	0.18 to 5.6
β_p	0.95	0.81	0.74	0.09 to 2.5
V_A (km sec^{-1})	43	42	17	18 to 88
M_A	10.7	10.1	4.8	4.4 to 20.0
Δ	-4°	---	38°	---
α	0.48	0.38	.40	0.05 to 2.8

TABLE 3

Plasma Properties in the Quiet Solar Wind ($300 \leq V \leq 350$ km sec^{-1})

Parameter	Average	σ	Median
B (gammas)	4.7	2.2	4.3
ϕ	137°	47°	---
θ	-3.2°	32.6°	---
N (p/cm^3)	8.3	3.6	7.2
T (°K)	4.6×10^4	2.6×10^4	4.1×10^4
ϵ	1.20	0.90	1.02
β_p	0.78	0.69	0.67
V_A (km sec^{-1})	36	16	33
M_A	10.7	5.0	10.1

REFERENCES

Ahluwahlia, H. S. and A. J. Dessler, Diurnal variation of cosmic radiation intensity produced by a solar wind, Planet. Space Sci. 9, 195 (1962).

Axford, W. I., Observations of the interplanetary plasma, Space Sci. Rev., 8, 331, 1968.

Bame, S. J., J. R. Asbridge, H. E. Felthauser, E. W. Hones and I. B. Strong, Characteristics of the plasma sheet in the earth's magnetotail, J. Geophys. Res., 72, 113, 1967.

Bame, S. J., J. R. Asbridge, A. J. Hundhausen and I. B. Strong, Solar wind and magnetosheath observations during the January 13-14, 1967, geomagnetic storm, J. Geophys. Res., 73, 5761, 1968.

Bame, S. J., J. R. Asbridge, A. J. Hundhausen, and M. D. Montgomery, Electron and proton temperatures in the disturbed solar wind (abstract), Trans. Am. Geophys. Union, 50, 301, 1969.

Burlaga, L. F. and K. W. Ogilvie, Heating of the solar wind, Astrophys. J., 159, 659, 1970a.

Burlaga, L. F., and K. W. Ogilvie, Magnetic and kinetic pressures in the solar wind, NASA-GSFC preprint X-692-70-208, 1970b.

Burlaga, L. F., K. W. Ogilvie, and D. H. Fairfield, Microscale fluctuations in the interplanetary magnetic field, Ap. J., 155, L171, 1969.

Carovillano, R. L., and G. L. Siscoe, Corotating structure in the solar wind, Solar Phys., 8, 401, 1969.

Coleman, P. J., L. Davis, E. J. Smith and D. E. Jones, The Polarity pattern of the interplanetary magnetic field during solar rotations 1798-1808, J. Geophys. Res., 72, 1637-1643, 1967.

Coon, J. H., Solar wind observations, in Earth's Particles and Fields, edited by B. M. McCormac, p. 359, Reinhold, New York, 1968.

Dessler, A. J., Solar wind and interplanetary magnetic field, Rev. Geophys., 5, 1, 1967.

Eviatar, A., and Michael Schulz, Ion-temperature anisotropies and the structure of the solar wind, Planet. Space Sci., 18, 321, 1970.

Fairfield, D. H., Bow Shock Associated Waves Observed in the Far Upstream Interplanetary Medium, J. Geophys. Res., 74, 3541-3553, 1969.

Fairfield, D. H. and N. F. Ness, Magnetic Field Measurements with the IMP-2 Satellite, J. Geophys. Res., 72, 2379-2403, 1967.

Fairfield, D. H., Average and unusual locations of the earth's magnetopause and bow shock, NASA-GSFC preprint X-692-70-452, 1970.

Gosling, J. T., J. R. Asbridge, S. J. Bame, and I. B. Strong, Vela 2 measurements of the magnetopause and bow shock positions, J. Geophys. Res., 72, 101, 1967.

Greenstadt, E. W., I. M. Green, G. T. Ionuge, A. J. Hundhausen, S. J. Bame, and I. B. Strong, Correlated magnetic field and plasma observations of the earth's bow shock, J. Geophys. Res., 73, 51-60, 1968.

Hirshberg, J. and D. S. Colburn, The interplanetary field and geomagnetic variations-a unified view, Planet. Space Sci., 17, 1183, 1969.

Hundhausen, A. J., Direct observations of solar wind particles, Space Sci. Rev., 8, 690, 1968.

Hundhausen, A. J., Composition and dynamics of the solar wind plasma, Rev. Geophys. Space Phys., 8, 729, 1970.

Hundhausen, A. J., J. R. Asbridge, S. J. Bame, H. E. Gilbert and I. B. Strong, Vela 3 satellite observations of solar wind ions: A preliminary report, J. Geophys. Res., 72, 87, 1967a.

Hundhausen, A. J., J. R. Asbridge, S. J. Bame, and I. B. Strong, Vela satellite observations of solar wind ions, J. Geophys. Res., 72, 1979, 1967b.

Hundhausen, A. J., S. J. Bame, and N. F. Ness, Solar wind thermal anisotropies, Vela 3 and IMP 3, J. Geophys. Res., 72, 5265, 1967c.

Hundhausen, A. J., S. J. Bame, J. R. Asbridge, and S. J. Sydoriak, Solar wind proton properties: Vela 3 observations from July 1965 to June 1967, J. Geophys. Res., 75 (25), 4643, 1970a.

Hundhausen, A. J., S. J. Bame and M. D. Montgomery, The large-scale characteristics of flare-associated solar wind disturbances, J. Geophys. Res., 75(25), 4631, 1970b.

Lazarus, A. J., and J. H. Binsack, Observations of the Interplanetary plasma subsequent to the July 7, 1966, proton flare, Ann. IQSY, 3,378, 1969.

Lazarus, A. J. Pioneer 6 and 7 observations of average solar wind properties (abstract), Trans Am. Geophys. Union, 51, 413, 1970. 1970.

Longmire, C. L., Elementary Plasma Physics, Interscience Publishers, New York, 1963.

Montgomery, M. D., S. J. Bame and A. J. Hundhausen, Solar wind electrons: Vela 4 measurements, J. Geophys. Res., 73, 4999, 1968.

Ness, N. F., Observed properties of the interplanetary plasma, Ann. Rev. Astron. Astrophys., 6, 79, 1967.

Ness, N. F., The Magnetic structure of interplanetary space, Proceedings 11th International Conference Cosmic Rays, Budapest 1969, 41-84, ed. by G. Bozoki et al.

Ness, N.F., and H. E. Taylor, Observations of the Interplanetary magnetic field July 4-12, 1966, Ann. IQSY, 3, 366, 1969.

Ness, N. F., and J. M. Wilcox, Solar origin of the interplanetary magnetic field, Phys. Rev. Let., 13, 461, 1964.

Ness, N. F., and J. M.Wilcox, Interplanetary sector structure, 1962-1966, Solar Physics, 2, 351-359, 1967.

Neugebauer, M. and C. W. Snyder, Mariner 2 observations of the solar wind, 1, Average properties, J. Geophys. Res., 71, 4469, 1966.

Neugebauer, M., and C. W. Snyder, , Mariner 2 observations of the solar wind, 2, Relation of plasma properties to the magnetic field, J. Geophys. Res., 72, 1823, 1967.

Ogilvie, K. W. Acceleration of Particles at Shock Waves in the Interplanetary Medium, Summer Institute for Astrophysics SUNY, 1970.

Ogilvie, K. W. and N. F. Ness, Dependence of the lunar wake on solar wind plasma characteristics, J. Geophys. Res., 74, 4123-4128, 1969.

Parker, E. N., Interplanetary Dynamical Processes, Interscience, New York, 1963.

Rosenberg, R. L., and P. J. Coleman, Jr., Heliographic Latitutde dependence of the dominant polarity of the interplanetary magnetic field, J. Geophys. Res., 74, 5611, 1969.

Scarf, F. L., J. H. Wolfe, and R. W. Silva, A plasma instability associated with thermal anisotropies in the solar wind, J. Geophys. Res., 72, 993, 1967.

Strong, I. B., J. R. Asbridge, S. J. Bame, H. H. Heckman, and A. J. Hundhausen, Measurements of proton temperatures in the solar wind, Phys. Rev. Lett., 16, 631, 1966.

Taylor, H. E., Sudden commencement associated discontinuities in the interplanetary magnetic field observed by IMP 3, Solar Phys, 6, 320, 1969.

Whang, Y. C. and N. F. Ness, Observations of the lunar mach cone, J. Geophys. Res., 75, 6002, 1970.

Wilcox, J. M., The interplanetary magnetic field: solar origin and terrestrial effects, Space Sci. Rev., 8, 258, 1968.

Wilcox, J. M. and N. F. Ness, Quais-stationary corotating structure in the interplanetary medium, J. Geophys. Res., 70, 5793, 1965.

Wilcox, J. M. and D. S. Colburn, Interplanetary Sector Structure in the Rising Portion of the Sunspot Cycle, J. Geophys. Res., 74, 2388-2392, 1969.

Wilcox, J. M. and D. S.Colburn, Interplanetary sector structure near the maximum of the solar cycle, J. Geophys. Res., 75, 6366, 1970.

FIGURE CAPTIONS

Figure 1 Relative geometry of Vela 3-IMP 3 satellites used to compute time for convection of interplanetary medium between the two satellites (see text).

Figure 2 Statistical distribution of interplanetary magnetic field magnitude and direction as observed by IMP 3 during 1965-1967, when simultaneous Vela 3 plasma data was available.

Figure 3 Statistical distribution of proton thermal energy density and magnetic field energy density as observed separately by Vela 3-IMP 3 during 1965-1967.

Figure 4 Statistical distribution of the ratio of magnetic field energy density to proton thermal energy density observed simultaneously by Vela 3-IMP 3 during 1965-1967.

Figure 5 Statistical distribution of Alfvén speed as derived from simultaneous Vela 3-IMP 3 data obtained during 1965-1967.

Figure 6 Statistical distribution of angular difference of proton thermal anistropy and magnetic field directions as observed simultaneously by IMP 3- Vela 3 during 1965-1967.

Figure 7 Statistical distribution of firehose instability parameter, α_p, as observed simultaneously by Vela 3-IMP 3 during 1965-1967.

Figure 8 Correlation of magnetic field intensity, B, with solar wind flow speed, V, as observed simultaneously by Vela 3-IMP 3 during 1965-1967.

Figure 9 Correlation of magnetic field intensity, B, with proton number density, N, as observed simultaneously by Vela 3-IMP 3 during 1965-1967.

Figure 10 Correlation of interplanetary magnetic field direction with solar wind flow speed, V, as observed simultaneously by Vela 3-IMP 3 during 1965-1967.

Figure 11 Correlation of solar wind proton β with solar wind flow speed, V, as observed simultaneously by Vela 3-IMP 3 during 1965-1967.

Figure 12 Correlation of average radial component of solar wind proton temperature, T_{rad}, with direction of interplanetary magnetic field, Φ_B, as observed simultaneously by Vela 3-IMP 3 during 1965-1967.

Figure 13 Superposed epoch graphs of solar wind flow speed, V, solar wind proton density, N, flow direction φ, proton temperature, T, and magnetic field intensity, B, observed for "well-defined" sectors in 1965-1967 as measured simultaneously by Vela 3-IMP 3 (see text).

Figure 14 Variation of 3 hour averages of plasma and field parameters V, N, T, B during solar rotation 1806 from 15 July to 10 August 1965 as observed simultaneously by Vela 3-IMP 3.

Figure 15 Variation of 3 hour averages of plasma and field paramters V, N, T, B during solar rotation 1807 from 11 August to 6 September 1965 as observed simultaneously by Vela 3-IMP 3.

Figure 16 Variation of 3 hour averages of plasma and field parameters V, N, T, B during solar rotation 1808 from 7 September to 2 October 1965 as observed simultaneously by Vela 3-IMP 3.

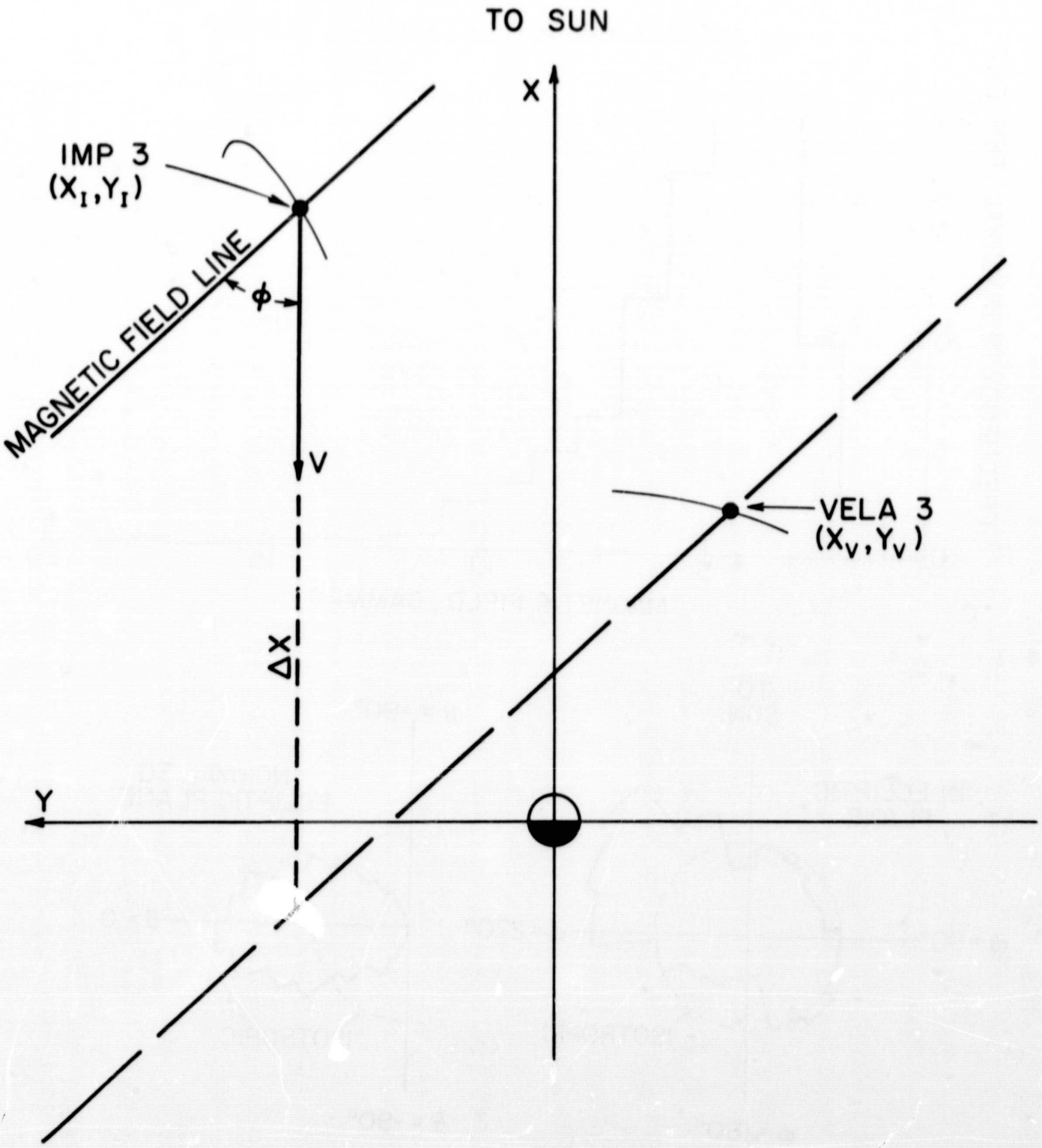
TO SUN
X
IMP 3
(X_I, Y_I)
MAGNETIC FIELD LINE
ϕ
V
VELA 3
(X_V, Y_V)
ΔX
Y

FIGURE 1

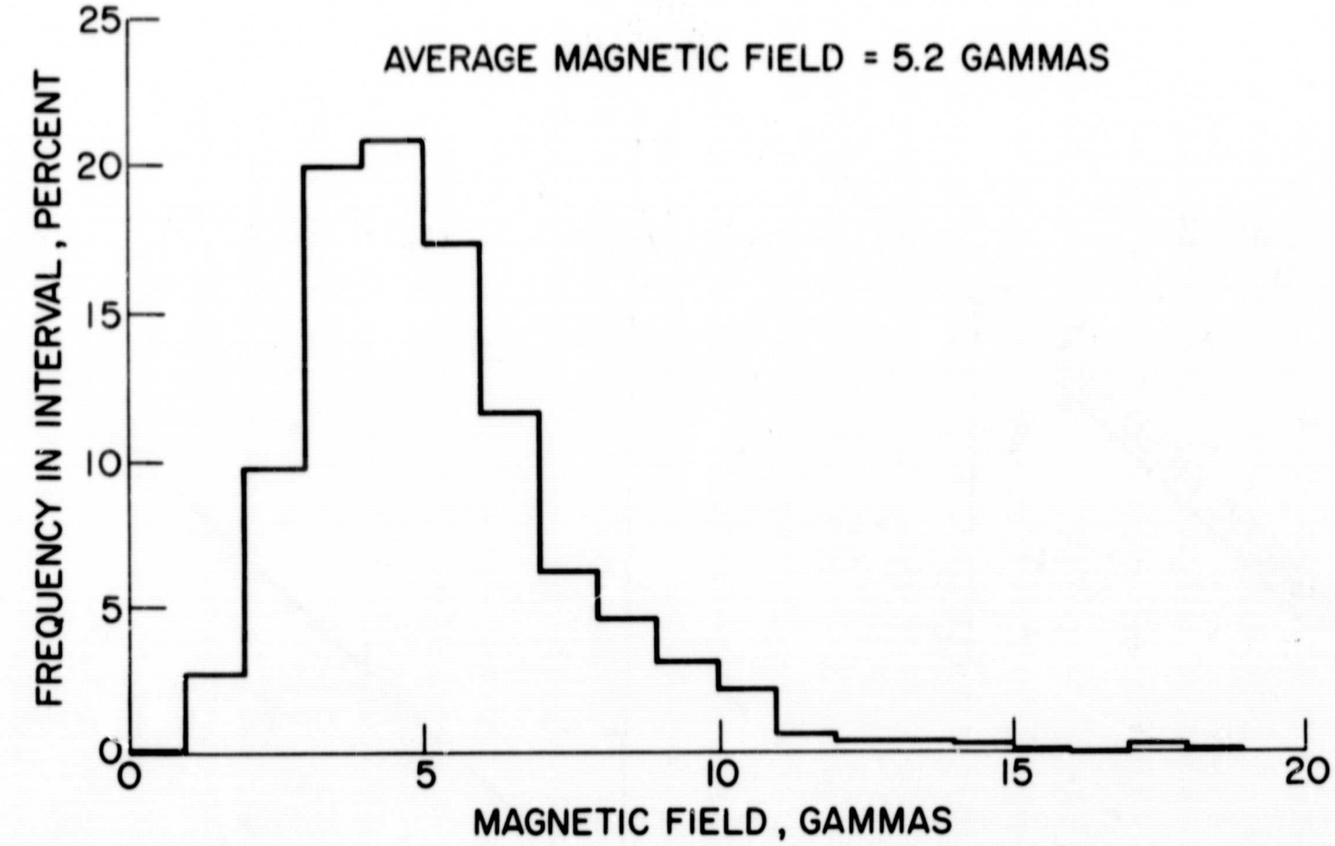
AVERAGE MAGNETIC FIELD = 5.2 GAMMAS
FREQUENCY IN INTERVAL, PERCENT
25
20
15
10
5
0
0
5
10
15
20
MAGNETIC FIELD, GAMMAS

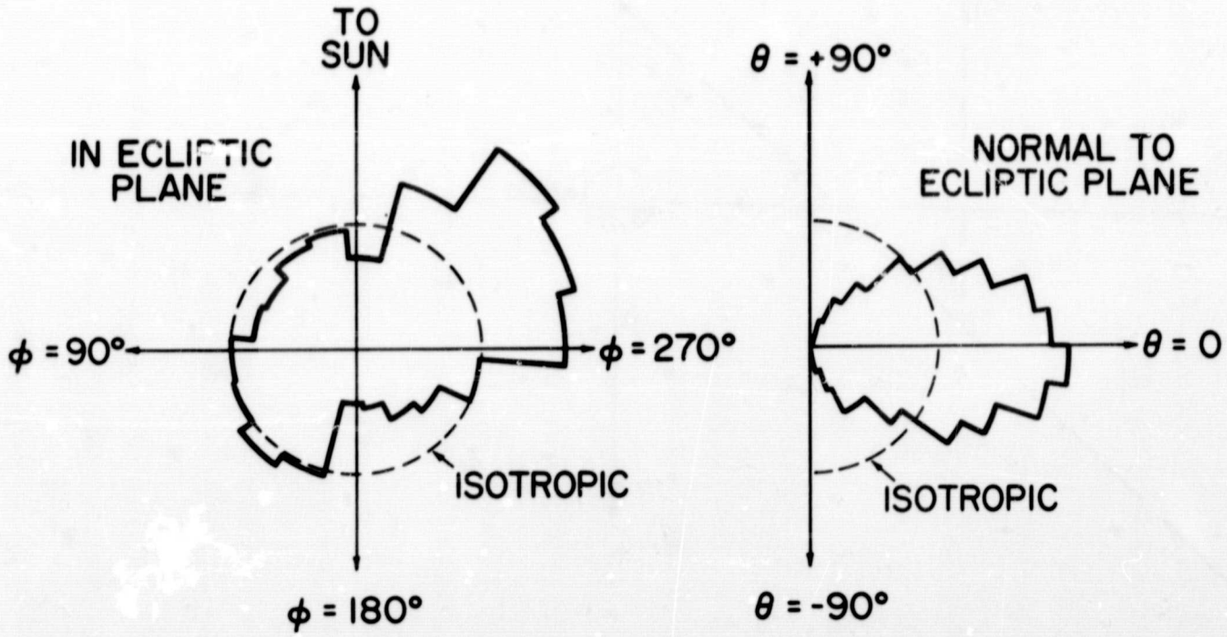
TO SUN
IN ECLIPTIC PLANE
φ = 90°
φ = 270°
ISOTROPIC
φ = 180°
θ = +90°
NORMAL TO ECLIPTIC PLANE
θ = 0
ISOTROPIC
θ = -90°

FIGURE 2

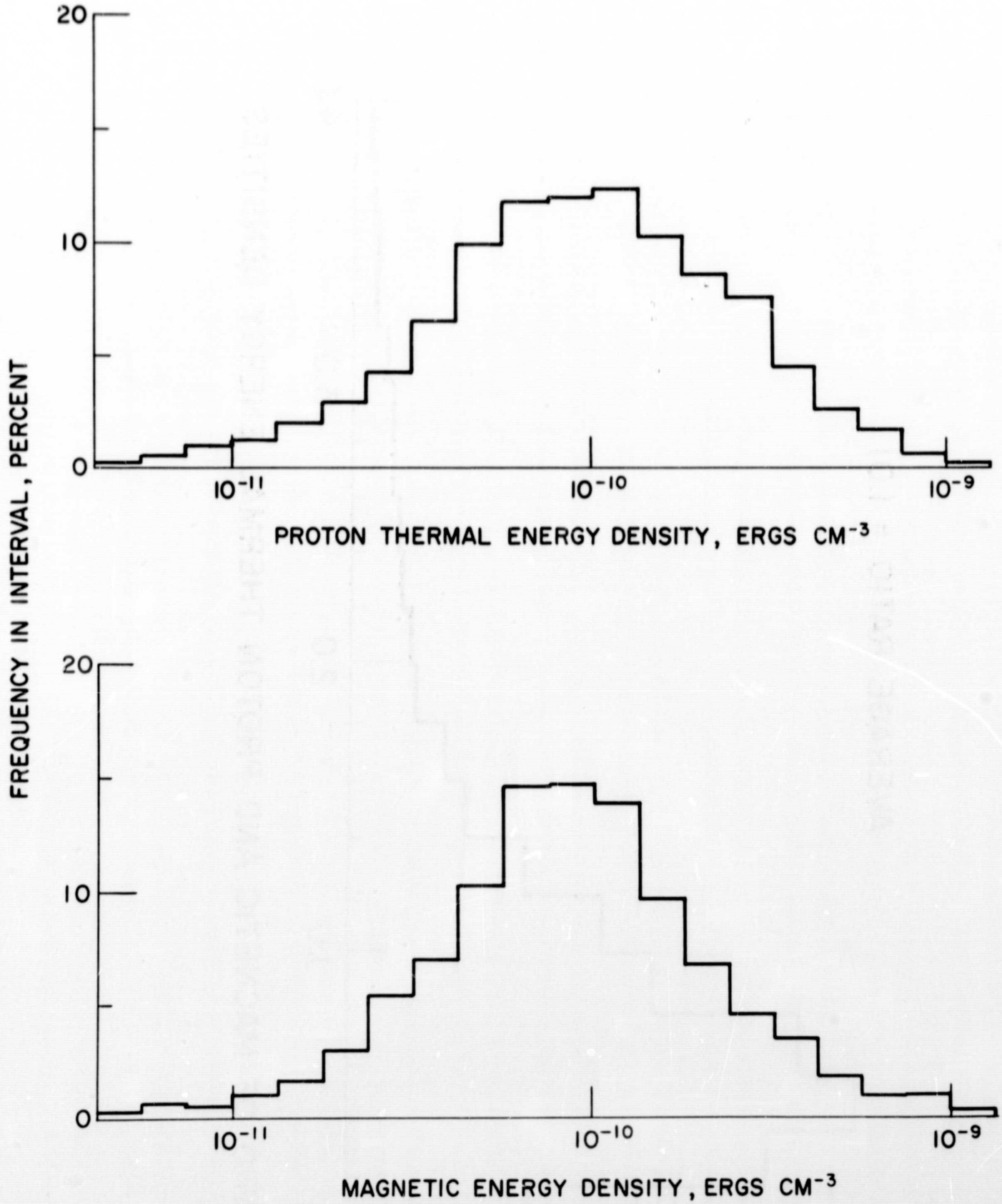
20
10
0
FREQUENCY IN INTERVAL, PERCENT
10^{-11}
10^{-10}
10^{-9}
PROTON THERMAL ENERGY DENSITY, ERGS CM^{-3}
20
10
0
10^{-11}
10^{-10}
10^{-9}
MAGNETIC ENERGY DENSITY, ERGS CM^{-3}

FIGURE 3

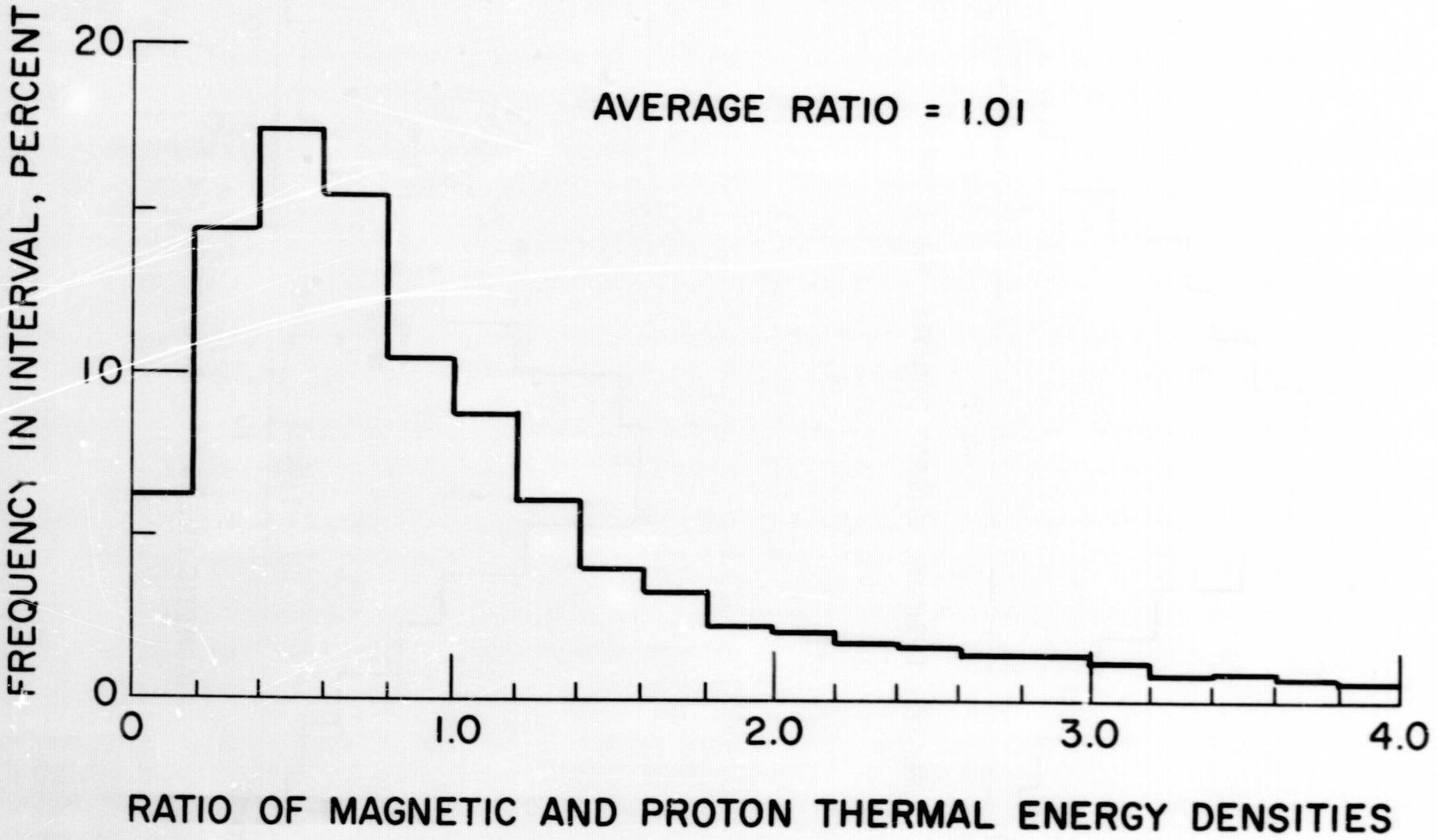
AVERAGE RATIO = 1.01
FREQUENCY IN INTERVAL, PERCENT
20
10
0
0
1.0
2.0
3.0
4.0
RATIO OF MAGNETIC AND PROTON THERMAL ENERGY DENSITIES

FIGURE 4

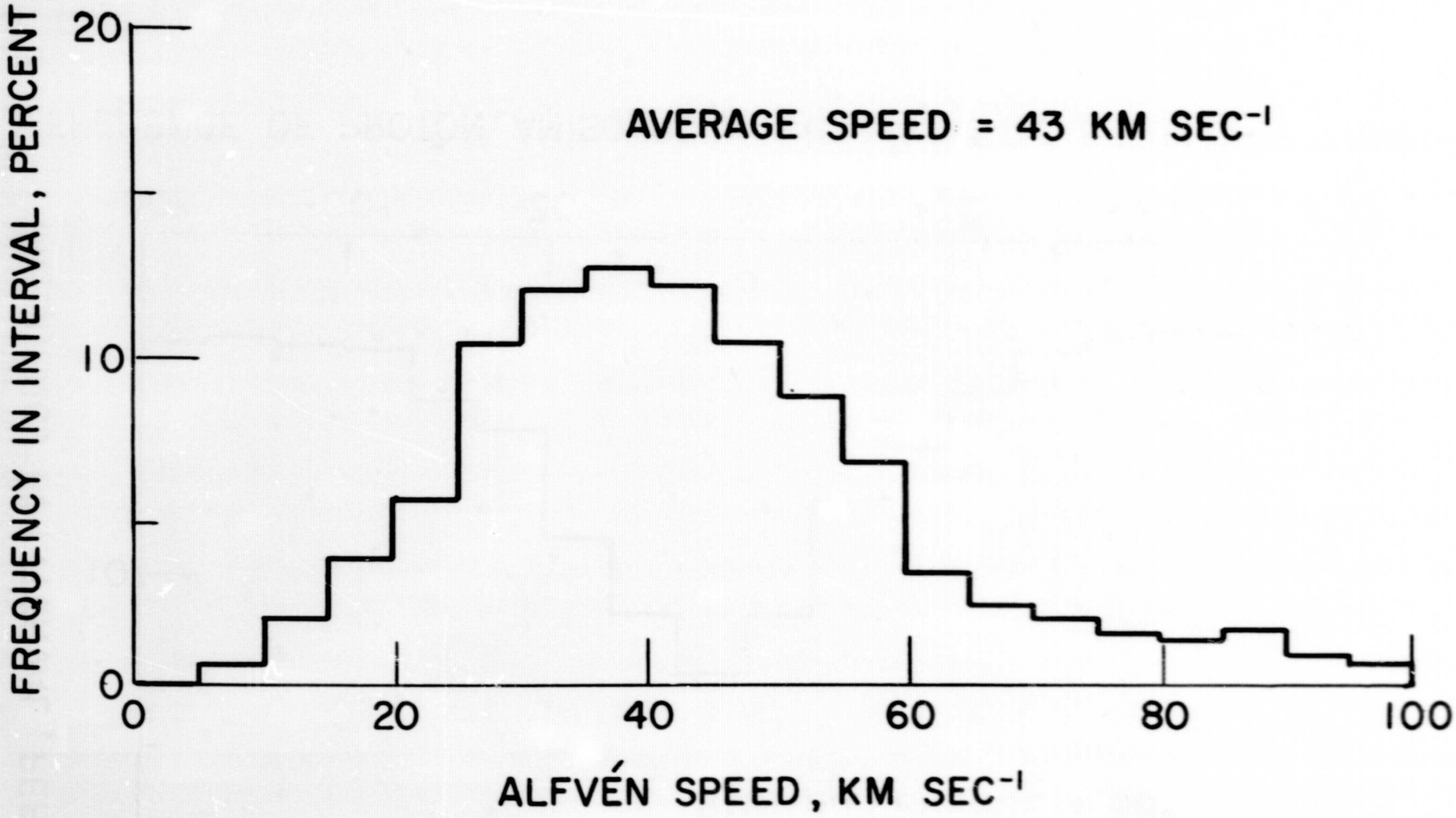
AVERAGE SPEED = 43 KM SEC⁻¹
FREQUENCY IN INTERVAL, PERCENT
20
10
0
0
20
40
60
80
100
ALFVÉN SPEED, KM SEC⁻¹

FIGURE 5

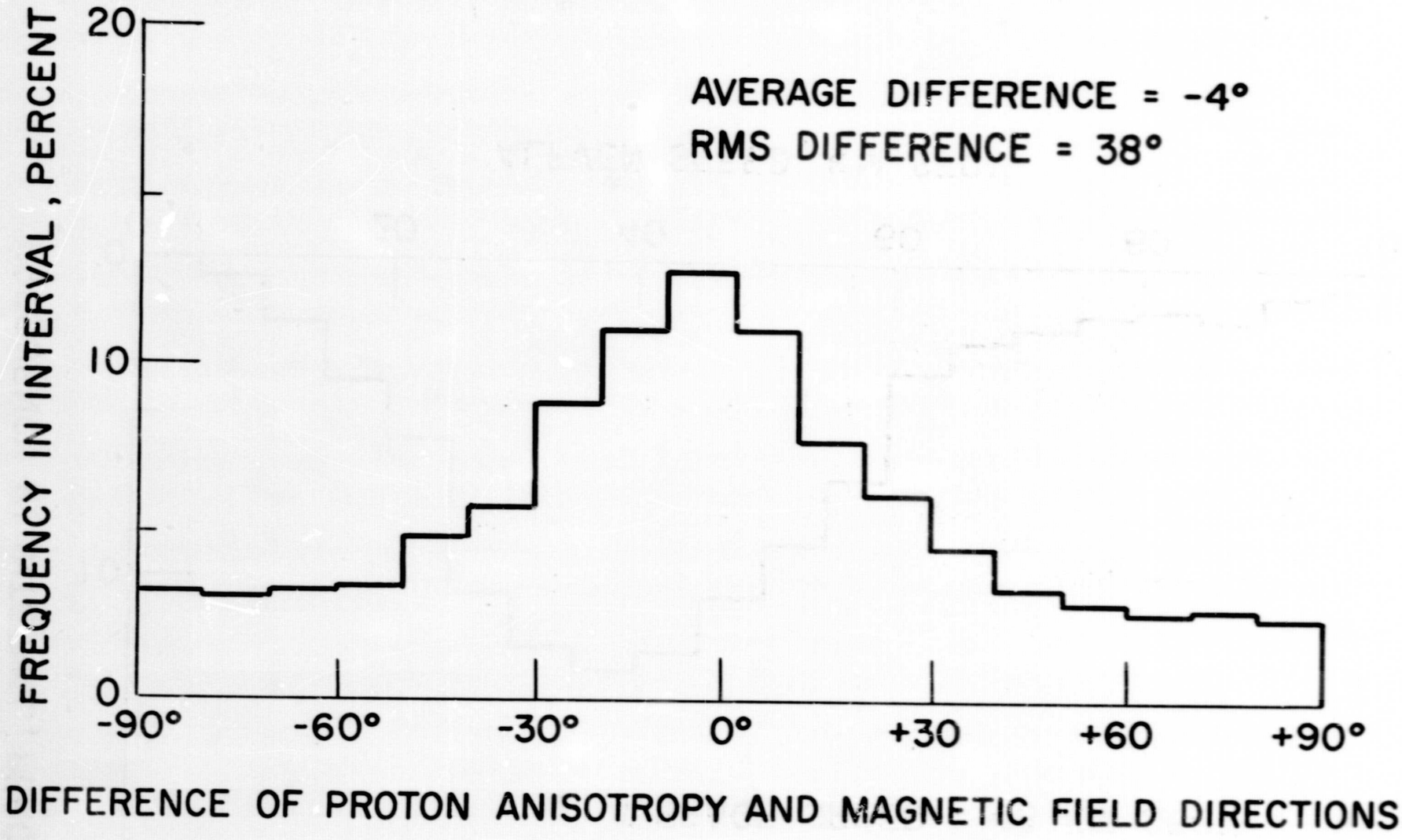
AVERAGE DIFFERENCE = -4°
RMS DIFFERENCE = 38°
FREQUENCY IN INTERVAL, PERCENT
20
10
0
-90°
-60°
-30°
0°
+30
+60
+90°
DIFFERENCE OF PROTON ANISOTROPY AND MAGNETIC FIELD DIRECTIONS

FIGURE, 6

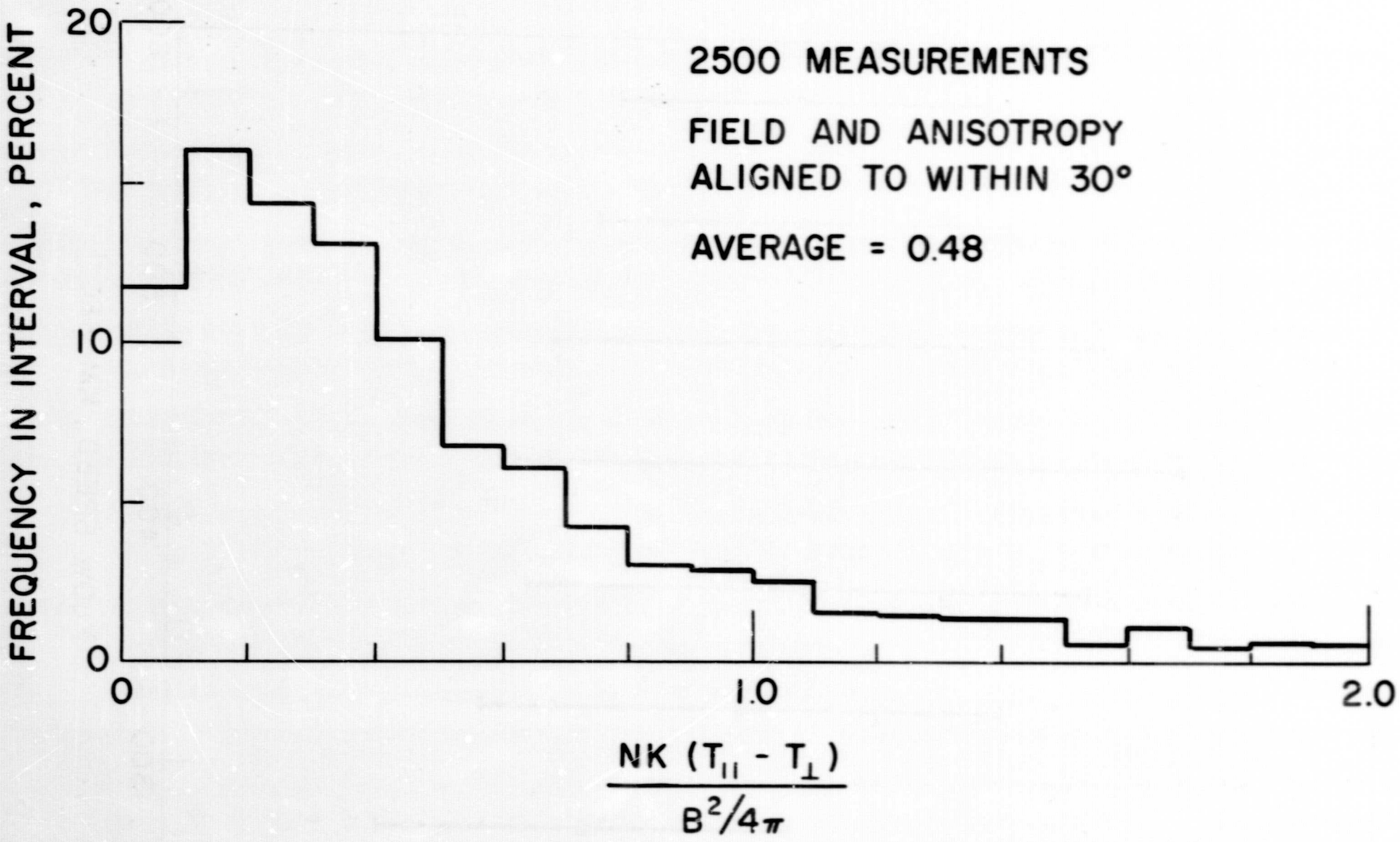
2500 MEASUREMENTS
FIELD AND ANISOTROPY
ALIGNED TO WITHIN 30°
AVERAGE = 0.48
FREQUENCY IN INTERVAL, PERCENT
20
10
0
0
1.0
2.0
NK (T11 - T⊥)
B²/4π

FIGURE 7

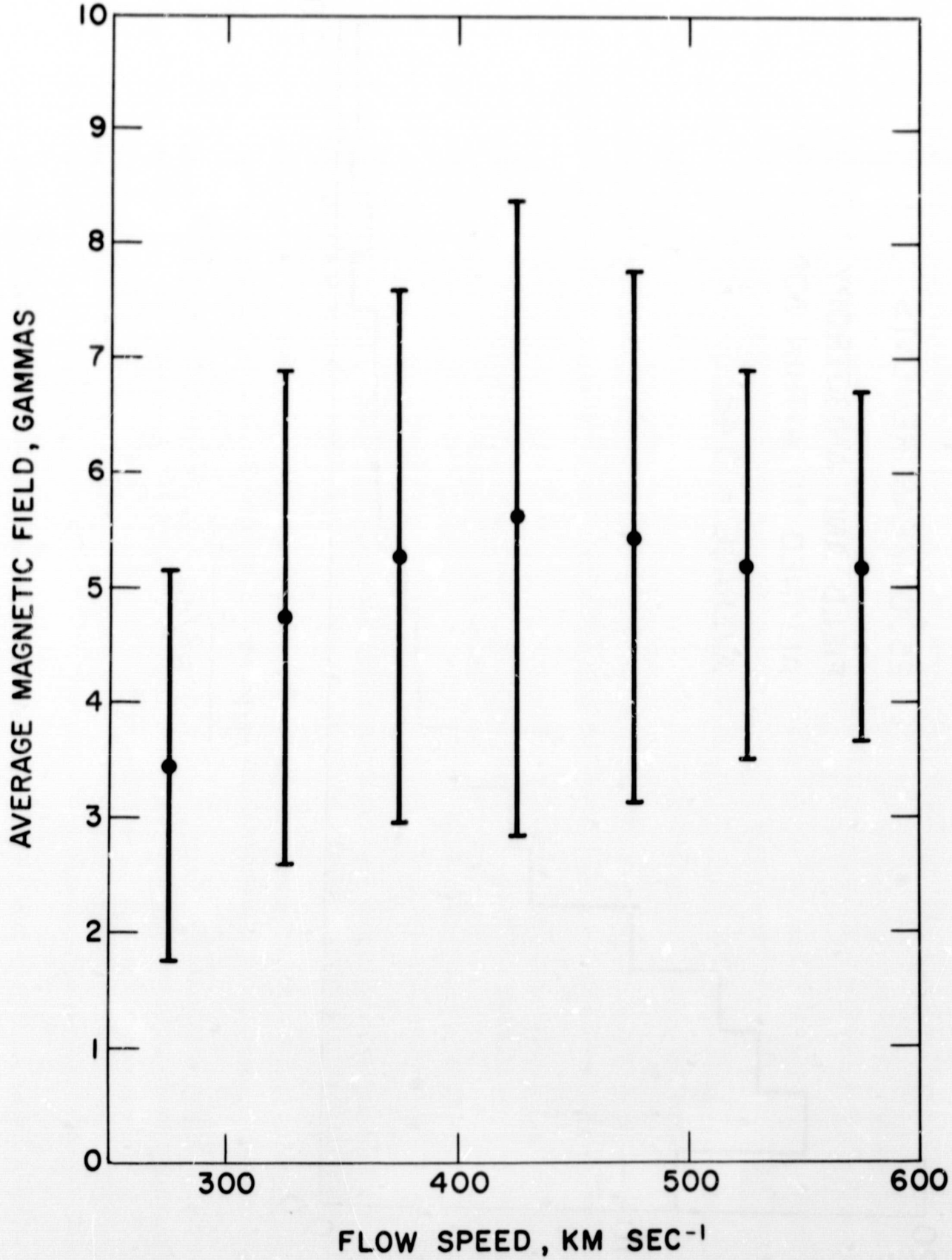
AVERAGE MAGNETIC FIELD, GAMMAS
0
1
2
3
4
5
6
7
8
9
10
300
400
500
600
FLOW SPEED, KM SEC⁻¹

FIGURE 8

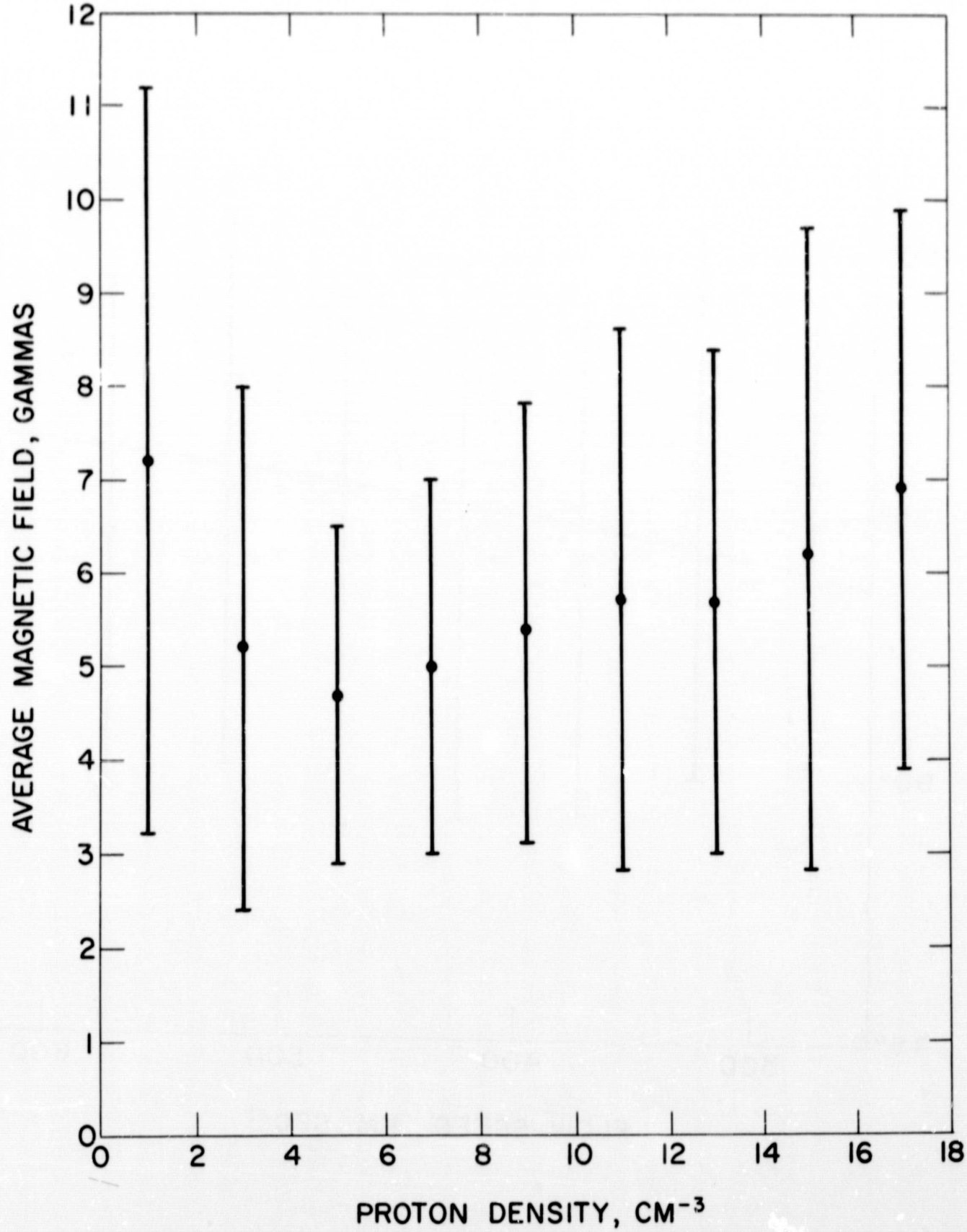
AVERAGE MAGNETIC FIELD, GAMMAS
PROTON DENSITY, CM^{-3}
0
1
2
3
4
5
6
7
8
9
10
11
12
0
2
4
6
8
10
12
14
16
18

FIGURE 9

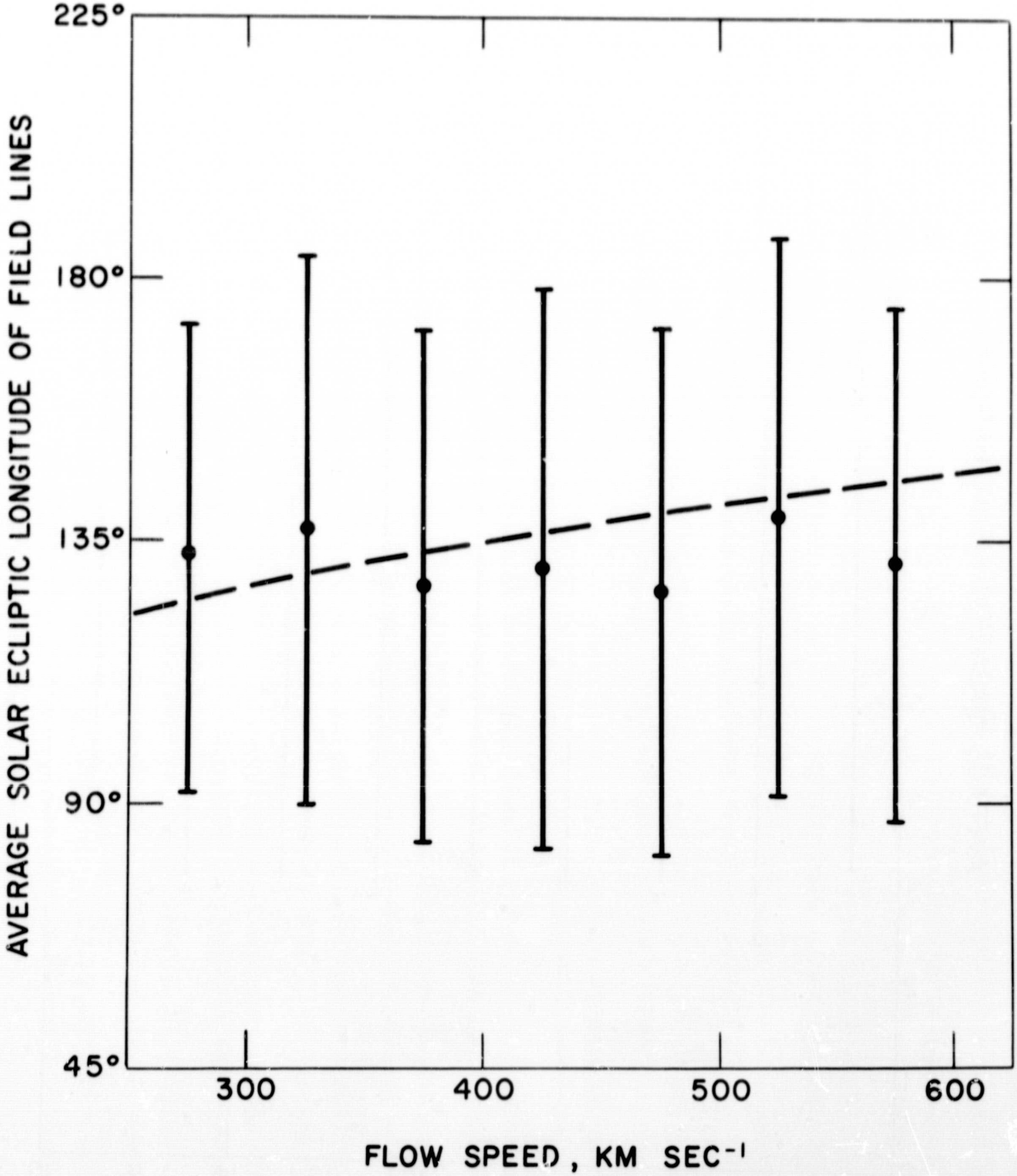
225°
180°
135°
90°
45°
AVERAGE SOLAR ECLIPTIC LONGITUDE OF FIELD LINES
300
400
500
600
FLOW SPEED, KM SEC⁻¹

FIGURE 10

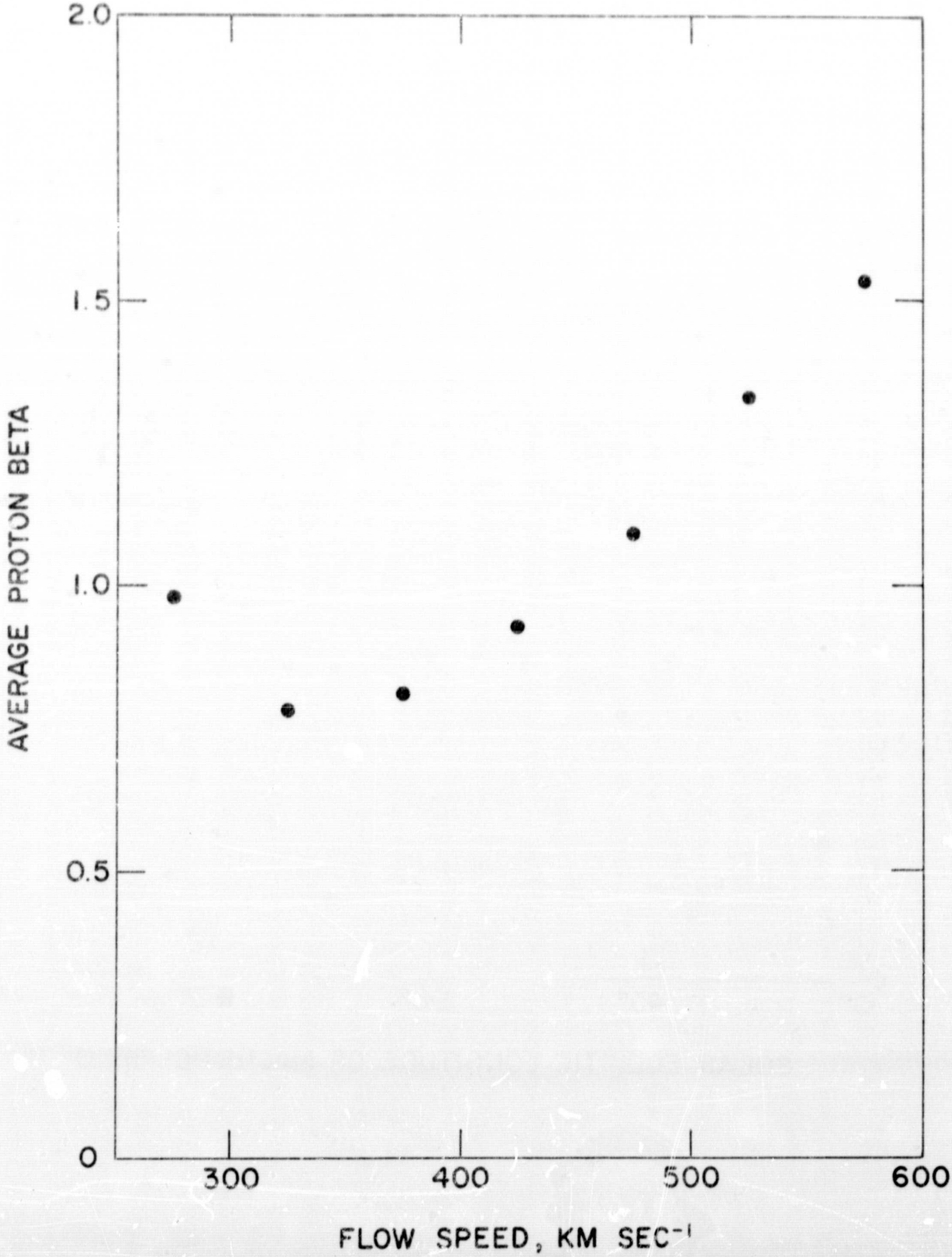
2.0
1.5
1.0
0.5
0
AVERAGE PROTON BETA
300
400
500
600
FLOW SPEED, KM SEC⁻¹

FIGURE 11

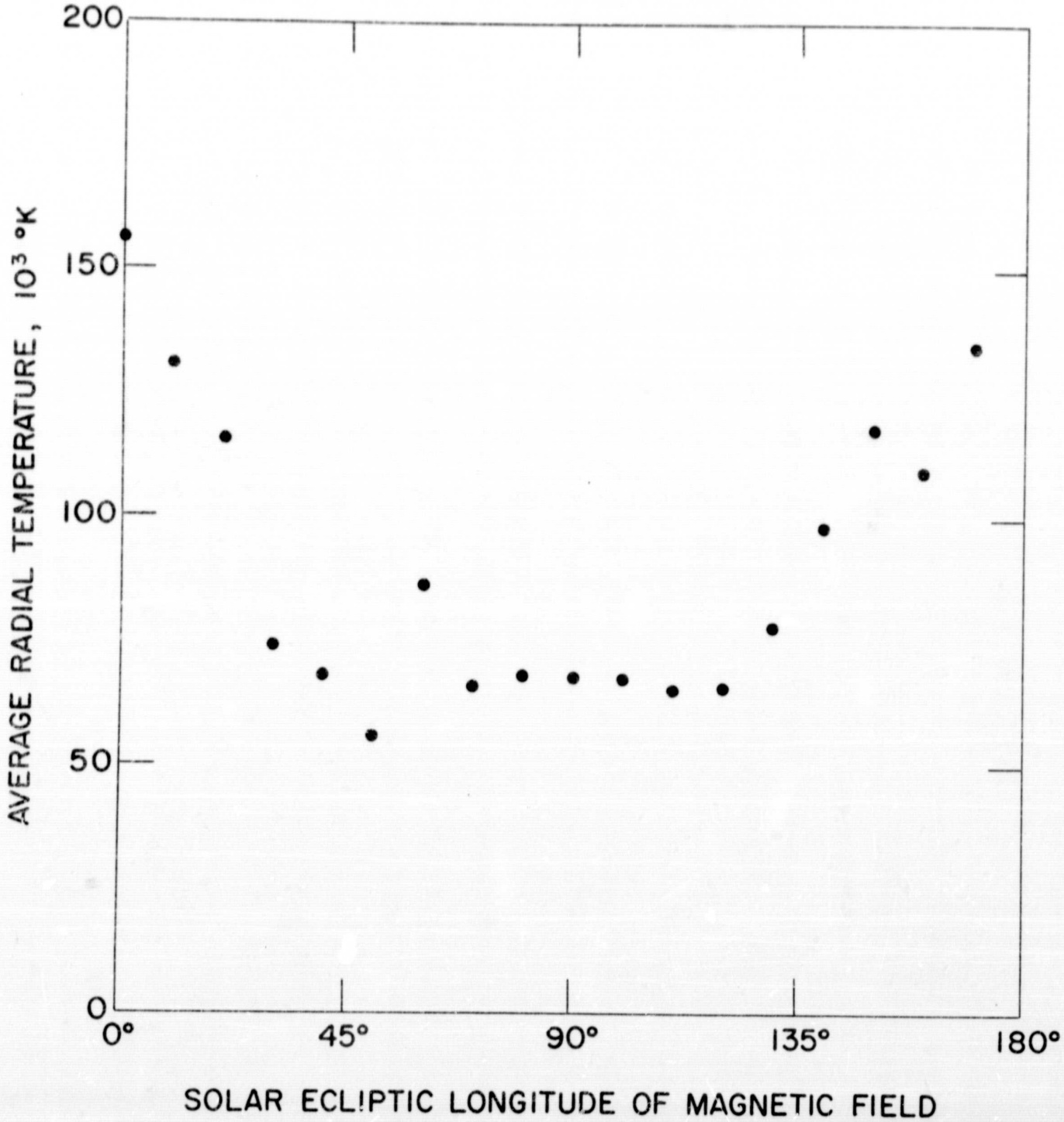
200
150
100
50
0
AVERAGE RADIAL TEMPERATURE, 10^3 °K
0°
45°
90°
135°
180°
SOLAR ECLIPTIC LONGITUDE OF MAGNETIC FIELD

FIGURE 12

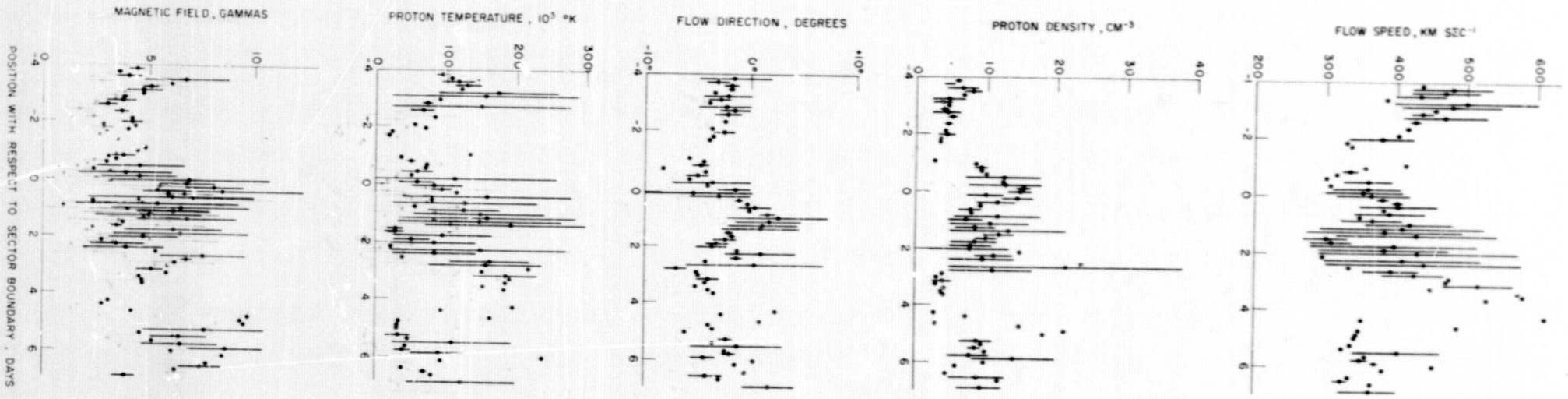
MAGNETIC FIELD, GAMMAS
PROTON TEMPERATURE, 10^3 °K
FLOW DIRECTION, DEGREES
PROTON DENSITY, CM^{-3}
FLOW SPEED, KM SEC^{-1}
POSITION WITH RESPECT TO SECTOR BOUNDARY, DAYS

FIGURE 13

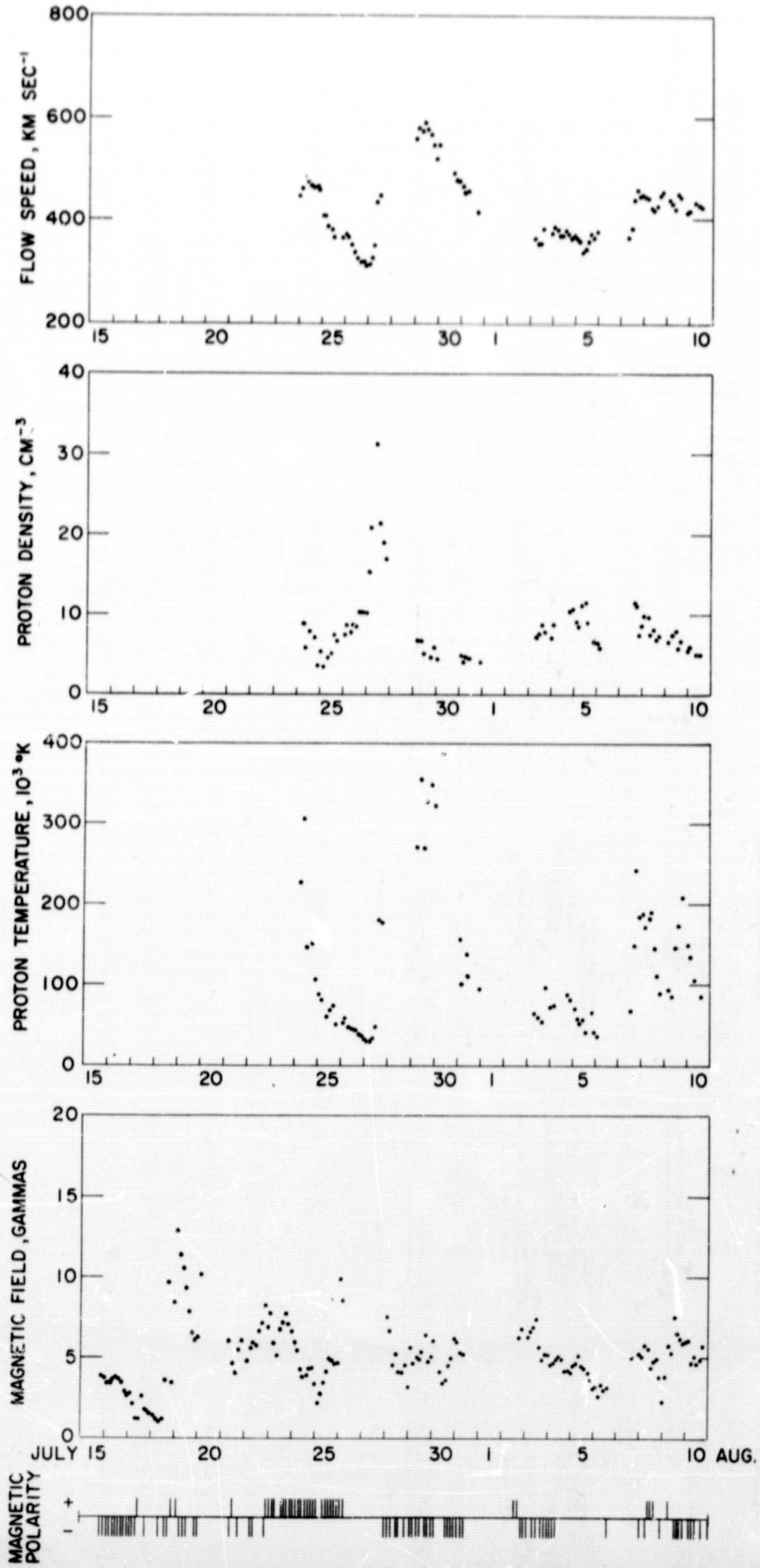
FLOW SPEED, KM SEC⁻¹
800
600
400
200
PROTON DENSITY, CM⁻³
40
30
20
10
0
PROTON TEMPERATURE, 10³ °K
400
300
200
100
0
MAGNETIC FIELD, GAMMAS
20
15
10
5
0
15
20
25
30
1
5
10
JULY
AUG.
MAGNETIC POLARITY
+
-

FIGURE 14

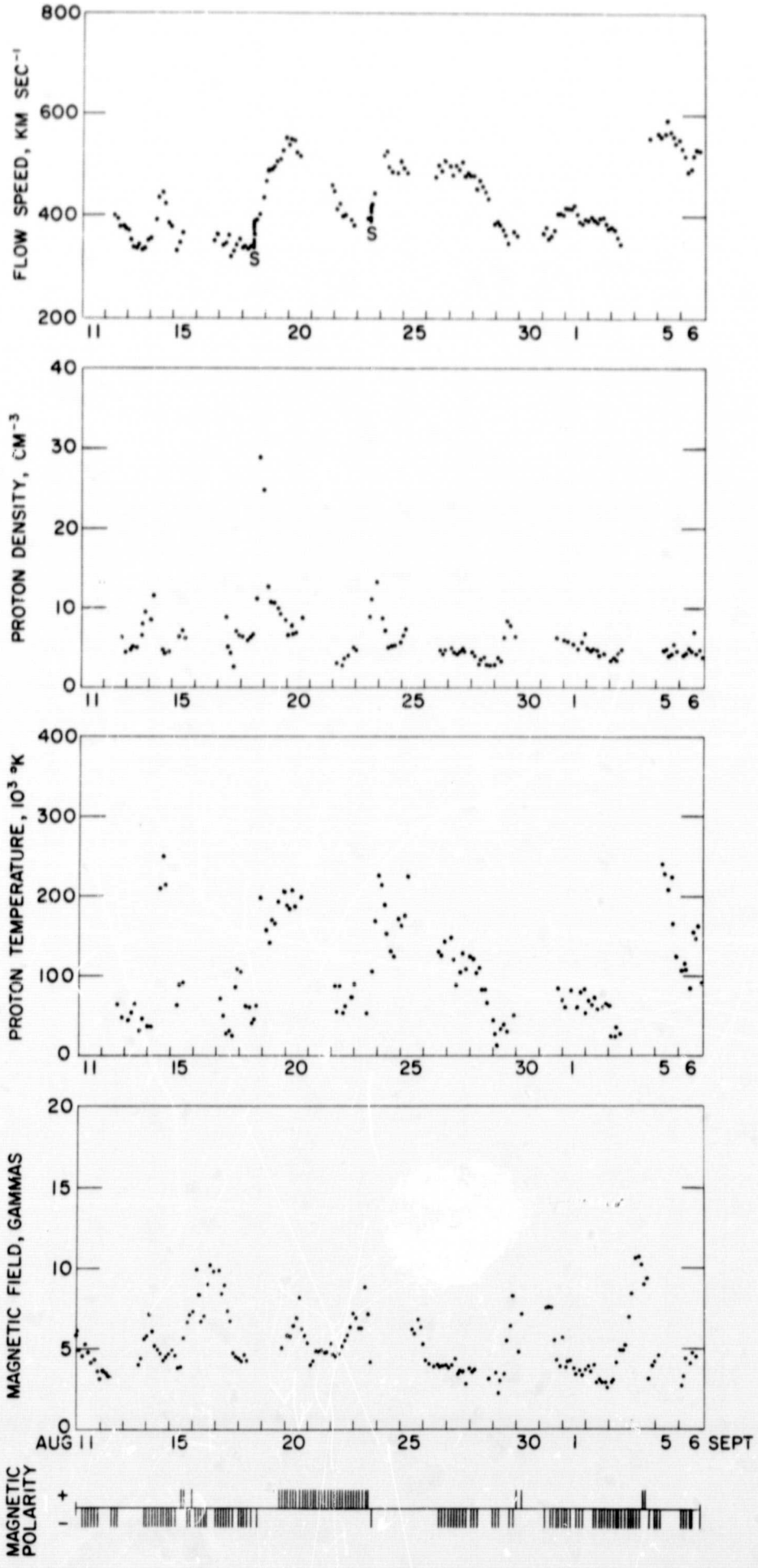
FLOW SPEED, KM SEC⁻¹
800
600
400
200
S
S
11
15
20
25
30
1
5
6
PROTON DENSITY, CM⁻³
40
30
20
10
0
PROTON TEMPERATURE, 10³ °K
400
300
200
100
0
MAGNETIC FIELD, GAMMAS
20
15
10
5
0
AUG
SEPT
MAGNETIC POLARITY
+
-

FIGURE 15

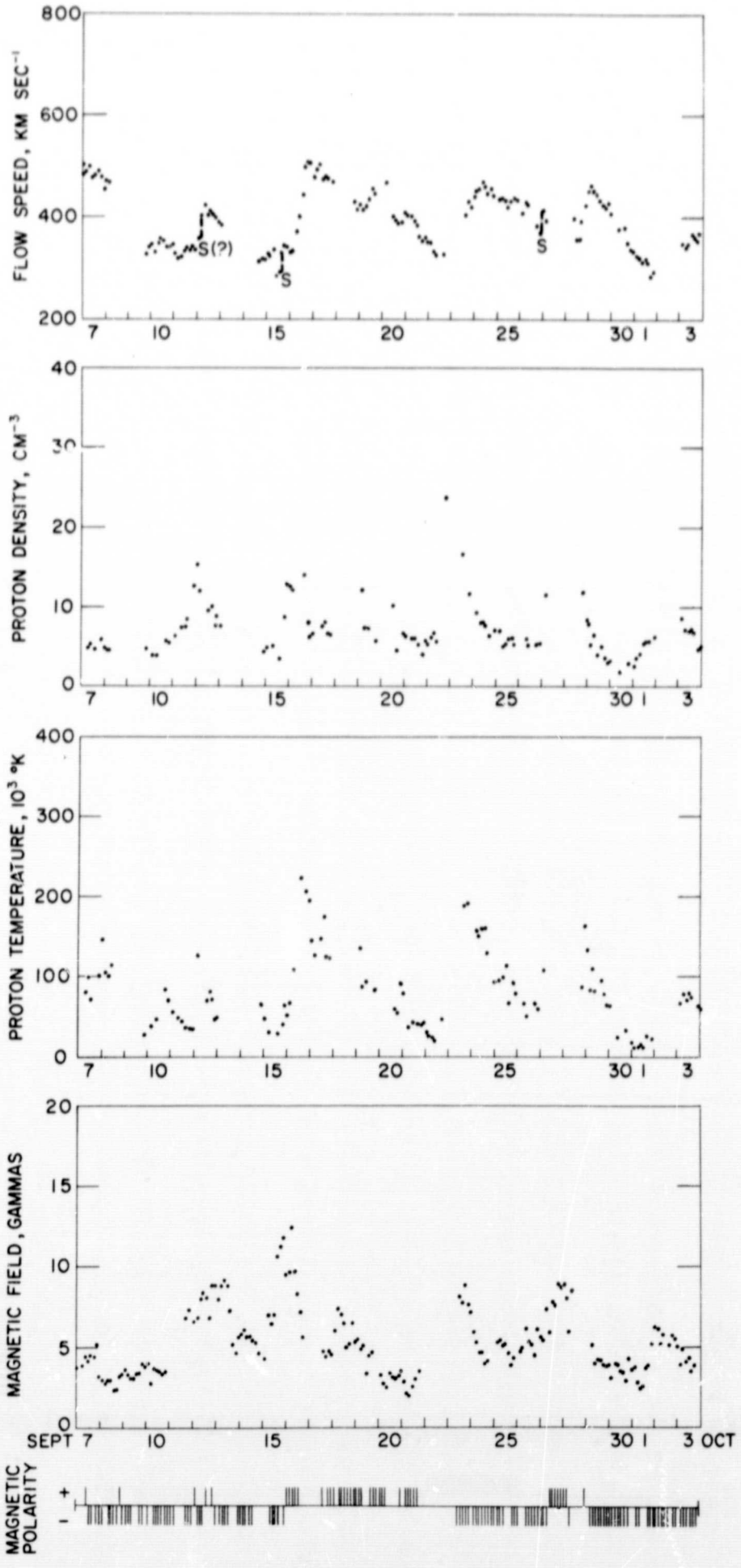
FLOW SPEED, KM SEC⁻¹
800
600
400
200
S(?)
S
S
7
10
15
20
25
30
1
3
PROTON DENSITY, CM⁻³
40
30
20
10
0
PROTON TEMPERATURE, 10³ °K
400
300
200
100
0
MAGNETIC FIELD, GAMMAS
20
15
10
5
0
SEPT
3 OCT
MAGNETIC POLARITY
+
-

FIGURE 16